M 2014

U.PORTO
FEUP FACULDADE DE ENGENHARIA
UNIVERSIDADE DO PORTO

Assessment of the Binding Properites of KtrA to ATP and ADP

JOÃO MIGUEL ANTUNES SANTOS
DISSERTAÇÃO DE MESTRADO APRESENTADA
À FACULDADE DE ENGENHARIA DA UNIVERSIDADE DO PORTO EM
BIOENGENHARIA

- This page was intentionally left blank. -

Faculdade de Engenharia da Universidade do Porto

Instituto de Ciências Biomédicas Abel Salazar

FEUP

U.PORTO

INSTITUTO DE CIÊNCIAS BIOMÉDICAS ABEL SALAZAR
UNIVERSIDADE DO PORTO

Assessment of the Binding Properties of KtrA to ATP and ADP

João Miguel Antunes Santos

Master Thesis
Submitted in partial fulfilment
of the requirements for the Degree of
Master of Science in Bioengineering,
at the Faculdade de Engenharia da Universidade do Porto
and Instituto de Ciências Biomédicas Abel Salazar

Supervisor: João Morais Cabral

June 2014

Abstract

KtrAB is the main K^+ transporter in many bacterial species. Deficiency on any of its composing subunits results in impaired K^+ uptake, which could be critical given the importance of this ion in the survival of bacteria.

The recent resolution of the structure of KtrAB complex provided new insight on the disposition of the transporter subunits as well as possible regulators of the activity of the complex. The estimated high affinity of the RCK domains of KtrA to adenine-containing ligands, namely ATP and ADP allied to observed conformational changes of the KtrA octameric ring upon binding of these metabolites, suggests a possible regulation mechanism involving shifts in the ATP/ADP ratio. Such regulation could be similar to what is observed for the P_{II} regulatory proteins. Defining the mechanism responsible for the transduction of KtrA conformational shifts into the opening of the pore and activation of the KtrAB complex composes the next big challenge for the full characterization of this transporter complex.

In order to continue to pursue the defined challenge, in this work I characterized some of the binding properties of KtrA to the adenosine-containing molecules ATP, ADP and AMP. I established a method to remove most of the ligand still bound to KtrA and assessed the ligand binding affinities using Isothermal Titration Calorimetry. The affinities of KtrA to ATP and ADP are similarly high, while AMP holds the lowest affinity of the three. The respective K_D values determined were 690 nM, 763 nM and 4 μM. I also performed the partial characterization of binding site residues mutant proteins with the objective of understanding the role of each mutated residue in the protein interaction with the ligands.

Full understanding of the complexity associated with KtrA binding to its ligands can only be accomplished by further investigation. Even though, the affinity values determined here should be considered as an important step towards the characterization of the KtrAB complex by further enabling the understanding of the mechanisms behind the regulation of KtrAB activation.

- This page was intentionally left blank. -

Acknowledgments

First of all, I can only express a profound gratitude to my parents and brother for their unconditional support and force throughout this challenging yet rewarding stage of my life. Also, to my closest friends for the incredibly great times we spent during the past few years.

I would like to specially acknowledge my thesis advisor and supervisor, Dr. João Morais Cabral, for promptly giving me the fantastic opportunity to develop my Masters Thesis in his lab and for all the guidance, support and advice he has given me ever since. In his lab, I had the chance to expand my knowledge and practical experience, and I am sure I leave this semester fully prepared to face the new challenges ahead.

I would also like to express my sincere gratitude to Ricardo Vieira-Pires, Andras Szollosi and Celso Duarte for their precious help and availability throughout the past six months. To them I owe most of the knowledge I acquired during the development of this project.

I leave a special ‘thank you’ to the Structural Biochemistry group for welcoming me and promptly helping my integration in the lab, as well as for all their support.

Last but definitely not the least, I am overwhelmingly grateful to Bárbara, who have always been there, specially in the difficult moments, tirelessly holding me back up no matter what.

To all, thank you so much.

- This page was intentionally left blank. -

Table of Contents

List of Figures

List of Tables

- This page was intentionally left blank. -

Glossary

ADP - Adenosine diphosphate

AMP – Adenosine monophosphate

ATP – Adenosine triphosphate

DTT - Dithiothreitol

HKT – High-affinity K^+ transporter

IPTG - Isopropyl-beta-D-thiogalactopyranoside

ITC – Isothermal Titration Calorimetry

K_D – Dissociation constant

K_m – Michaelis-Menten constant

KTN – K^+ transport nucleotide-binding domain

Ktr – K^+ transporter

LB – Luria-Bertani

M – Transmembrane helix

P – Pore loop

Trk – transport of K^+

NAD^+/NADH – Nicotinamide adenine dinucleotide

RCK –Regulate conductance of K^+ domain

TCEP - Tris(2-carboxyethyl)phosphine

WT – Wild type

- This page was intentionally left blank. -

Chapter 1

Introduction

1.1. Physiologic importance of K^+

The potassium ion (K^+) is the most abundant cation present in the cytoplasm. It participates in crucial aspects in living organisms such as the control of the cell growth and tolerance to osmotic pressure [1, 2].

K^+ concentrations are usually larger in the cytoplasm than in the extracellular surroundings. This cation plays an essential part in the physiology of the cell by contributing to the control of the electrical membrane potential, the maintenance of the internal pH, the regulation of the turgor pressure or the balance of anionic charges [1-3].

Membrane K^+ transporters are, thus, vital to ensure the proper K^+ concentration inside the cell. An important superfamily of K^+ transporters is the Trk/Ktr/HKT transporter family [1, 4]. This family comprises highly homologous K^+ transporters that can be found in bacteria, fungi or plants but not in animals. The uptake of K^+ is possible due to the hyperpolarized state originated by the excretion of H^+ and Na^+ by pumps in the cell membrane, which creates a favourable gradient to the entrance of the positively charged K^+ ion [1]. Na^+, despite its higher toxicity to the cell, is often used as a replacement when K^+ availability is low. In fact, many of these membrane proteins are also able to permeate Na^+, possibly by a symport mechanism with K^+ [1, 2].

1.2. Trk/Ktr/HKT transporter family

The uptake of K^+ is mediated by K^+ transporters, some of which are grouped in the Trk/Ktr/HKT transporter family. This family of potassium transporters is represented by several homologue membrane proteins divided in four distinct groups (figure 1): the fungal Transport of K^+ (Trk); the bacterial Trk; the bacterial K^+ transporter (Ktr); and the High-affinity K^+ transporter (HKT) in plants [1]. There are many other classes of K^+ transporters and channels, such as voltage-gated channels and K^+ uptake ATPases that will not be discussed here.

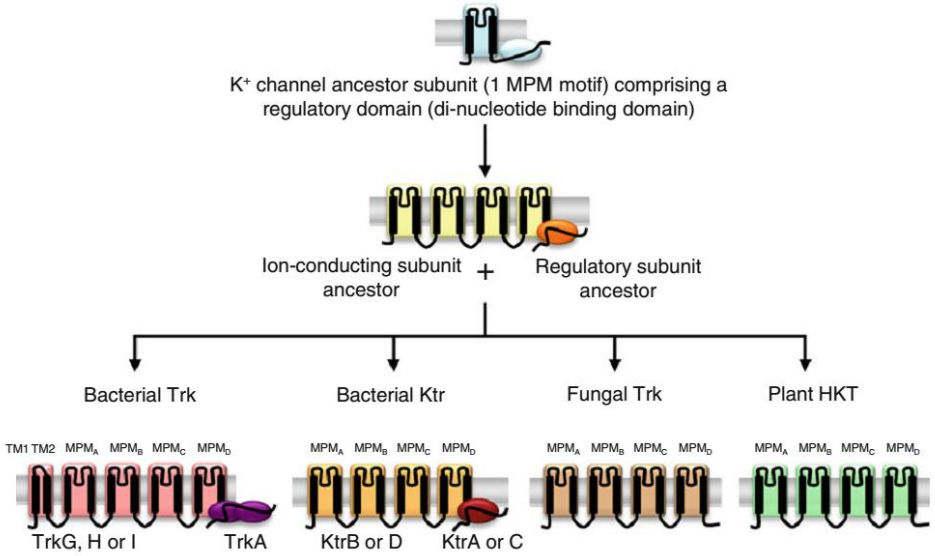

Figure 1 - Schematic representation of proposed Trk/Ktr/HKT transporter family evolution. Multiple gene duplication and fusion events of the K+ channel ancestral subunit, composed of one MPM motif and a regulatory domain, resulted in an ancestral K+ transporter composed of a single-gene coded ion-conducting subunit and a regulatory subunit. Four different groups arose from this common ancestor: the bacterial Trk, bearing two extra transmembrane domains in the N-terminal of their ion-conducting subunit and a regulatory subunit with two dinucleotide-binding sites; the bacterial Ktr, also formed by two subunits, the four MPM motifs composed transmembrane pore and a regulatory subunit; the fungal Trk and the plant HKT, both single subunit systems with the four MPM motifs forming the transmembrane pore. The regulation mechanisms of the latter transporters remain unknown. Adapted from [1].

1.2.1. Structural organization

Structurally, these transporters are composed by four MPM repeats (M stands for transmembrane helix, and P for a hairpin structure, or Pore loop). A scheme of such structures is depicted in figure 1 [1, 5, 6]. These motifs are arranged radially, with the transmembrane hydrophobic repeats protecting the P loops, which point inwards; the central axis of this structure defines the ion pore. The disposition of the four P loops is vital for the activity of the transporter, since these structures form the ion selectivity filter [5].

The importance of the P loops in ion selectivity and in the efficiency of K^+ uptake was proposed in several studies. There, the researchers described a relationship between the highly conserved glycine residues in the Trk/Ktr/HKT transporter family and the essential glycines present in the selectivity filter of K^+ channels [4, 5, 7-10]. This was confirmed by mutagenic studies where mutations of the conserved glycine residues in the P loop resulted in diminished or impaired selectivity and permeability of K^+ and/or Na^+ [8-10].

Some evidence suggest that these transporters arose from a common ancestor [5]. This precursor was the result of the assembling of 4 subunits, each with only one MPM repeat, and a regulatory domain. The K^+ transporter ancestor would have evolved, by gene duplication and fusion, into the transporters comprising the four MPM domains (figure 1) [5].

Both bacterial Trk and Ktr are multiple subunit systems. In addition to the ion-conducting transmembrane subunit, these protein complexes also possess a cytoplasmic regulatory subunit, TrkA and KtrA, respectively. The regulatory subunits are composed by one or more nucleotide-binding regions: the "K^+ transport, nucleotide binding" (KTN) or the KTN homologue "regulate conductance of K^+" (RCK) domains [3, 11, 12]. The mechanisms by which TrkA and KtrA mediate the activity of the pore are yet to be determined, although it is

known that structural rearrangements and nucleotide binding play a significant role in the control of the pore permeability [6, 13]. These regulatory subunits are thought to have been derived from a C-terminal regulatory domain in the ancestor transporter [5].

Contrarily, the HKT and the fungal Trk are single subunit systems, formed only by the ion-conducting subunit [1].

1.2.2. Functional properties

The transporters comprised in the Trk/Ktr/HKT family not only allow the uptake of K^+ alone (called K^+ uniport) but have also been described to permit the co-transport of Na^+ or H^+ alongside K^+ (Na^+-K^+ symporters and H^+-K^+ symporters). Examples of symporters include the HKT and bacterial Trk, respectively [1, 4].

Currently, two main models are used to describe the mechanism that controls the transport of ions through these transporters: the alternating-access model and the channel-like long pore model.

According to the first model, the transporter switches between two different conformations, thus oscillating the ion-binding sites between the extracellular and intracellular faces. Given that this behaviour is very similar to enzymes, Michaelis-Menten kinetics can apply, and the transport may be dependent of affinity constants and ligand saturation [2, 14].

The other model describes the pore as a long and narrow structure with multiple ion-binding sites along its extension. Through the pore, ions must flow in a single-file and occupy the binding sites sequentially [8]. As they enter the pore, the K^+ ions are partially dehydrated with rehydration occurring inside the cytoplasm [4]. The two models do not need to be taken as exclusive of one another. In fact, it is likely that a mix between the two models can occur. In any case these two should always be taken into account as possible ion permeation mechanisms [1].

1.3. KtrAB

The KtrAB transporter is a bacterial Ktr transporter known as a complex of two proteins: the ion-conducting transmembrane subunit KtrB and the regulatory subunit composed of RCK domains, KtrA [3, 15, 16].

The KtrAB complex was first described by Nakamura, *et al* [3] as a novel type of K^+-uptake system in *Vibrio alginolyticus*. This group stated the existence of two adjacent genes, *ktrA* and *ktrB* that encoded a peripheral membrane protein with a predicted molecular mass of 23 804 Da, later named KtrA, and a transmembrane protein similar to previously described NtpJ from *Enterococcus hirae* K^+ transport system [17], with a predicted molecular mass of 49 675 Da, KtrB [3]. The KtrAB transporter family has, later, been characterized in a wide number of bacteria [3, 18].

In *B. subtilis*, two different sets of Ktr transporters are described: the KtrAB and KtrCD (KtrC is equivalent to KtrA and KtrD to KtrB) [16]. The main difference between these two

transporters is their apparent affinity to K^+, higher for KtrAB (K_m ~ 1 mM) than for KtrCD (K_m ~ 10 mM). Furthermore, whereas the genes encoding the KtrA and KtrB subunits are transcriptionally organized in the same operon, the KtrC and KtrD genes seem to be expressed independently from one another [16]. Interestingly, upon deletion of one subunit (KtrA or KtrB), survival in low salinity medium was found to diminish, although the expression of the remaining subunit was not impaired, indicating that the high affinity K^+ uptake depends on the correct assembly of the KtrAB complex [3]. The K^+ uptake by the KtrAB complex was shown to be dependent of Na^+ [18] and ATP [19].

Early biochemical data obtained from cross-linking and light scattering/size exclusion chromatography studies led to the idea that the KtrB subunit is organized as a homodimer [15] while crystallographic assays of isolated KtrA have shown its organization in an octameric ring [20]. These previous studies were confirmed by the recent resolution of the KtrAB structure, where the KtrB homodimer is shown to interact with the face of a cytoplasmic KtrA octameric ring (figure 2) [6].

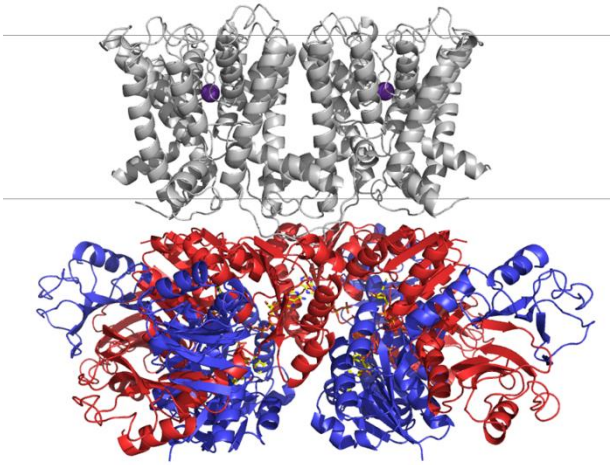

Figure 2 – Cartoon of the KtrAB structure. Grey structures represent the KtrB homodimer with a K^+ ion (purple sphere) inside the pore. At the top is the extracellular space; the membrane is represented by the two grey lines involving the transmembrane KtrB pore. The KtrA octameric ring is represented in the cytosolic side of the membrane. Each of the four dimers is composed by a blue and a red monomer. ATP bound to the N lobes of KtrA subunits are shown in yellow. Figure obtained from the *Structural Biochemistry* group database in IBMC.

Unlike K^+ channels, where the ion-conducting domain and the RCK containing subunit are part of a single polypeptide, in KtrAB the interactions between the two proteins forming the complex are mediated by two different types of contact: tip-contacts and lateral-contacts [6].

In the tip-contact, the apexes of the KtrB homodimer, namely the loop separating the first two MPM repeats (D1 and D2) of each subunit, interact with two opposite KtrA subunits. [6].

The lateral-contacts involve the C-terminus tails of each KtrB subunit. This 18 residue long feature interacts at the membrane-cytoplasm interface with KtrA residues burying a total of 600 $Å^2$ of surface area. Furthermore, the C-terminus tail of each KtrB monomer is determinant in the stability of the KtrB homodimer. In fact, the interaction between neighbouring KtrB monomers mediated by the C-terminus tail was impaired upon truncation of its last 10-15 residues and the protein failed to dimerize [15].

The two contact regions help to stabilize the KtrAB complex, thus maintaining a fully functional state of the K^+ transporter. This was confirmed by growth complementation assays using proteins with mutated residues involved in these contacts. Bacteria bearing these mutants did not survive in media with low K^+ concentration.[6]

1.2.3. KtrB

The ion-conducting subunit, KtrB, is a transmembrane protein composed, as already described, of four repeats (D1-D4) with a total of eight transmembrane motifs disposed around a cation selective pore (figure 3) [5]. The four repeats sequences generally differ among each other, aside from the conserved glycine filter regions that compose the selective pore [15]. In fact, this feature is responsible for the main characteristic associated to this subunit – its selective ion conduction – and could be considered equivalent to the active site in an enzyme [21].

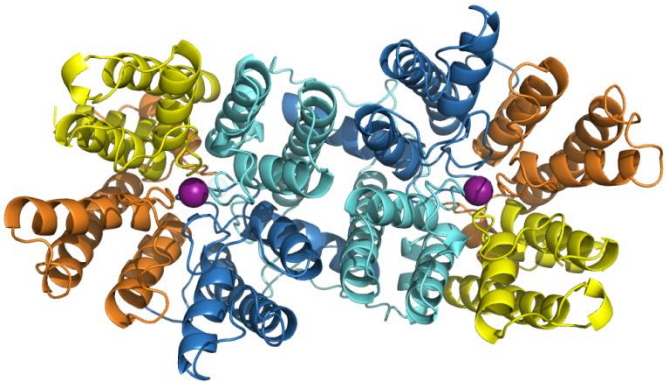

Figure 3 - Extracellular view of KtrB homodimer. Repeats D1 to D4 are shown respectively in yellow, orange, blue and cyan. K^+ ions going across the selectivity filter are represented as purple spheres. The KtrA octameric ring situated in the cytosolic end of the KtrB homodimer has been omitted. Figure obtained from the *Structural Biochemistry* group database in IBMC.

The properties of KtrB are also affected by an intramembranous loop composed by the residues linking the two transmembrane motifs of the D3 repeat (mostly glycines, alanines and serines). This loop is localized between the selectivity filter and the cytoplasmic pore, probably functioning as a gate for the control of the ion flux [6, 22].

Cytoplasmic loops of variable sizes connect the four repeats and usually extend several residues (15-36) into the cytoplasm [15].

1.2.4. KtrA

The KtrA regulatory subunits comprising RCK domains are positioned at the cytoplasmic face of the membrane. These subunits are arranged in an octameric ring, also described as a tetrameric assembly of dimers, with the N (amino) lobes of each subunit forming the interior of the ring whereas the C (carboxy) lobes face the cytoplasm [3, 6, 19].

The *B. subtilis* KtrA monomer is composed of a total of 222 amino acid residues and has a molecular weight of 24 880 g/mol. Its extinction coefficient, ε, when absorbing radiation with a wavelength of 280nm is 16 410 $cm^{-1}M^{-1}$ [properties calculated using the online tool Peptide Property Calculator by Northwestern University][23].

KtrA was shown to play an important role in the control of ion selectivity and transport rate of the Ktr systems, although the details by which the KtrA functions are yet to be clarified to this date [8]. The most accepted model is that ion flux is modulated through a gate-open mechanism based on conformational changes induced by the binding of a ligand [21]. How a conformational change in the KtrA octameric ring is transmitted to the KtrB homodimer is still not clear.

RCK domains are present in many K^+ transporters and, since the binding pocket residues are usually not conserved, a variety of ligands have been described to bind to these domains [21]. In fact, there is evidence that the RCK domains from the *E. coli* TrkA subunit bind nicotinamide dinucleotide (NAD^+) [24] and that the RCK domains from MthK channel bind Ca^{2+} [25]. The majority of RCK ligands remain unknown, though.

KtrA ligand-binding sites are located in the N lobe, on the inner rim of the octameric ring. KtrA binds adenine-containing ligands such as NADH/NAD^+ [12] and ATP, ADP or AMP [6, 19, 20]. Curiously, competition assays demonstrated that the affinity of KtrA to ATP and ADP is much higher than for NAD^+, leaving the notion that the first two could be the main ligands mediating KtrA conformational changes [19, 20]. However, the true dissociation constant (K_D) for ATP binding is yet to be determined. While Albright *et al* [20] determined a K_D of approximately 600 nM, Kröning *et al* [19] calculated a K_D of about 9 μM. This discrepancy may be due to major differences in the two approaches. For instance, while a truncated form of KtrA was used in the first study [20], the second group used a full-length KtrA [19]. Other possible causes may be the use of KtrA proteins from different bacterial species or the use of different methods for determining binding affinities. The ligand-mediated activation model by conformational changes has recently been supported by crystallographic experiments. There, KtrA conformation was shown to differ depending on the binding of ATP or ADP [6]. In these studies, the KtrA structure bound to ATP adopted a square-shaped ring with equal distances between opposing RCK domains (figure 4a). The substitution of ATP for ADP resulted in a broader diamond-shaped ring with one diagonal distance, measured between opposing subunits, increasing by around 12-16 Å, while the other remained practically unchanged (figure 4b). These results show, thus, a contraction of the KtrA octameric ring upon binding of ATP [6]. Furthermore, it has been shown that increasing ATP concentrations

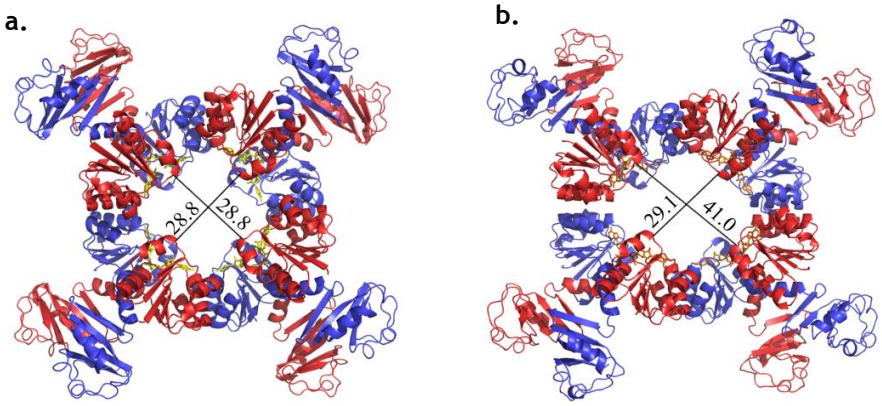

Figure 4 - Structure of the isolated KtrA octameric ring, either ATP-bound (a) or ADP-bound (b). Each of the four dimers is represented by two monomers in red and blue. The N lobes of each monomer are disposed towards the interior of the ring whereas the C lobes face the cytoplasm. ATP molecules are shown in yellow and ADP molecules are represented in orange. The distances shown were measured between two glutamic acid (E) residues in position 39 of opposing subunits and are represented in Å. Figure obtained from the *Structural Biochemistry* group database in IBMC.

lead to an increase in ion flux of KtrAB [6, 19]. These results indicate that the activation of KtrAB and associated opening of KtrB happen as a consequence of a contraction in the KtrA octameric ring.

Despite the importance of ATP binding in the activity of the KtrAB complex, there is no evidence of ATP hydrolysis, meaning that the transporter does not act as an ATPase [19].

Curiously, despite the discrepancy in the estimation of the K_D values for the binding of ATP, both values are much lower than the usual total cytosolic concentration of this metabolite in bacteria (9.6 mM in *Escherichia Coli* [26]). This has clear implications for the physiological mechanism of KtrAB regulation since, theoretically, the protein is constantly saturated with ligand in the cell. Such evidence should be carefully analysed. It is likely that the concentration of free ATP is lower than the total concentration of this metabolite. Furthermore, the K_D value for the assembled KtrAB complex is likely to be different from the values calculated for the KtrA subunit alone [19, 20]. Possibly, the physiological regulation of KtrAB is based on the competition between ATP and ADP for the RCK binding-sites. Consequently, the conformational switch of KtrA could occur as a function of the ratio between these two metabolites.

There are several metabolites with cytosolic concentrations higher than the K_m of the respective substrate-enzyme and to which competition based regulation have been reported [26]. A famous example of a protein family regulated in a similar fashion is the P_{II} protein family [27, 28]. The activation of these transduction proteins involved in the regulation of nitrogen metabolism is highly dependent on the ATP/ADP ratio inside the cell, as well as the cytoplasmic concentration of α-ketoglutarate [28].

1.4. Aim of the Project

Understanding how binding of ATP and ADP regulates the activity of KtrAB is an important objective in the characterization of this transporter complex. In fact, the extent to which the interaction with these two ligands mediates the conformational changes in KtrA and how these changes are transferred to the KtrB pore is still unclear.

The careful determination of the binding properties of ATP and ADP to KtrA will provide new insight on how the cytosolic regulatory protein changes its conformation and controls KtrAB activation. Therefore, the main objective of my work was the determination of the binding properties using Isothermal Titration Calorimetry. In particular the existence of cooperativity between binding sites in the same octamer would indicate that interactions occur between the eight binding sites of the KtrA octamer.

Given the already mentioned high binding affinities for ATP and ADP, determination of the binding properties of KtrA might be a problem. This results from incomplete depletion of ligand from all the KtrA binding sites leading to a competition with titrated ligands. Several attempts to remove the ligand bound to KtrA binding sites have been made without success, since either ligand removal was not efficient or the protein was destabilized in solution. In this project I developed a method to efficiently remove ligands bound to KtrA without apparently destabilizing the protein.

At the same time, a set of binding site residues mutants were obtained with the objective of characterizing the role of the mutated residues in the interaction with the ligands. Features like solubility, structural disposition and binding properties for ATP and ADP were assessed.

Finally, I crystallized the AMP-bound KtrA protein to assess the conformational effect of AMP binding.

1.5. Outline

This document is divided into five chapters. After being presented with a general view of the scientific background supporting this project and its objectives in **Chapter 1 – Introduction -**, the reader will find in **Chapter 2 – Materials and Methods** - all the methodology used. In **Chapter 3 – Results –** all the relevant results are described. The implications of the results obtained during the project are discussed and analysed in **Chapter 4 – Discussion**. Finally, the main results are highlighted in **Chapter 5 – Conclusions –** as well as the prospects and future work.

Chapter 2

Materials and Methods

2.1. Protein expression and purification

2.1.1. Bacteria transformation

Competent *E. coli* BL21 (DE3) cells were transformed with the KtrA gene containing plasmid pET24dKtrA. Competent cells stored at -80ºC were defrosted and 75ng of the plasmid were added to the cells. After a 30 minute incubation in ice, bacteria were heat-shocked during 1 minute at 42ºC. Following the addition of 900 µl of Luria-Bertani (LB) broth, bacteria cells were incubated for 1 hour at 37ºC. Competent cells were later centrifuged during 3 minutes at a speed of 2 000xg and the bacteria containing pellet was resuspended in 200 µl of LB. The transformed bacteria were transferred onto LB-agar (Sigma-Aldrich) containing petri dishes, supplemented with kanamycin (FORMEDIUM™) at 50 µg/ml.

2.1.2. Induction of KtrA over-expression

Bacteria transformed with the KtrA containing plasmid were grown in 4L flasks (AFORA) containing 1L of LB broth supplemented with Kanamycin (50 µg/ml) at 37ºC until an optical density (at 600 nm) of 0.6 was reached. KtrA over-expression was induced for ~14-16 h after addition of 500 µM of IPTG and 2.0% ethanol, at 20ºC.

2.1.3. Anion-exchange chromatography

After over-expression occurred, bacteria cells were pelleted for 20 minutes at a speed of 3 985xg, at 4ºC, in the JLA-8.1000 rotor (Beckman Coulter), using the Avanti J26XPI (Beckman Coulter) ultracentrifuge. Half the pellet obtained was immediately processed while the other half was stored at -20ºC for future KtrA purification. Cell lysis was done in Lysis Buffer (50 mM Tris-HCl pH 7.5, 50 mM KCl) supplemented with the protease inhibitors Leupeptin (1 µg/ml, Sigma-Aldrich), Pepstatin (1 µg/ml, Sigma-Aldrich) and PMSF (1mM, Sigma-Aldrich). The cell lysis was performed using the high pressure homogenizer EmulsiFlex-C5 (AVESTIN). Lysate was spin-cleared during 45 minutes at 35 000xg, at 4ºC, in the JA-25.50 rotor (Beckman Coulter), using the Avanti J26XPI ultracentrifuge. The resulting supernatant was loaded into a 5 ml HiTrap Sepharose Q HP (GE Healthcare) anion exchange column prewashed

with water and Low salt Buffer (50 mM Tris-HCl pH 7.5, 50 mM KCl, 5 mM DTT) attached to an ÄKTA purifier UP-10 (GE Healthcare). KtrA was eluted using a KCl concentration gradient formed by the Low salt buffer and a High salt Buffer (50 mM Tris-HCl pH 7.5, 1 M KCl, 5 mM DTT), with 100% of high-salt solution reached after 22 ml. Under a flow rate of 0.7 ml/min, 1 ml fractions corresponding to the first peak of elution profile (see Appendix A.1.) were collected, pooled and incubated with an ADP-agarose resin (Innova Biosciences) overnight at 4 °C. ADP-agarose resin beads were washed thoroughly with Wash Buffer (50 mM Tris-HCl pH 8.0, 150 mM KCl, 1mM TCEP (Sigma-Aldrich)) and protein was eluted in the same Wash Buffer supplemented with either 5 mM ADP or ATP or 50 mM AMP (Na-salts, Sigma-Aldrich).

2.1.4. Size-exclusion chromatography

Affinity-purified KtrA was concentrated to ~3 mg/ml using Macrosep Advance centrifugal devices (Pall Corporation) and further purified by size exclusion chromatography in a Superdex-S200 10/300 GL 25 ml column (GE Healthcare), attached to the FPLC System (Pharmacia Biotech LKB) and equilibrated with Gel Filtration Buffer (50 mM Tris-HCl pH 7.5, 150 mM KCl, 5 mM DTT). Size-exclusion chromatography was performed at 4ºC, using a flow rate of 0.5 ml/min and a chart-recorder recording speed of 1 cm/ml. KtrA fractions were collected at the previously defined elution volume of ~12.5 ml. The elution profile is represented in Appendix A.2. KtrA in solution was supplemented with 1 mM adenine-nucleotide from a 100 mM stock in 1 M Tris-HCl pH 7.5, or immediately submitted to dialysis, depending on the experiment planned.

The ADP-agarose resin was regenerated using Guanidine Hydrochloride (6M) and stored at 4ºC in Wash Buffer supplemented with sodium azide (0.02%) for future utilization.

2.2. Dialysis

KtrA in solution was transferred to a washed 10 kDa dialysis membrane (Spectra/Por) and dialysed in 250 ml of the appropriate Dialysis Buffer. Dialysis time and Dialysis Buffer substitutions were adapted depending on the experiments planned.

2.2.1. Extensive dialysis

Extensive dialysis was performed using the D4 dialysis buffer (150 mM K^+ PO_4^{3-} pH 8.0, 5 mM DTT). The dialysis buffer was substituted a total of four times, over four days. When extensive dialysis preceded ITC experiments, DTT was removed from D4 dialysis buffer during the fourth change, at least one day before the ITC experiment.

2.3. ATP quantification

ATP quantification was performed using the bioluminescence ATP detection kit ENLITEN ATP Assay System (Promega).

For both the validation experiments and the plotting of standard calibration curves, the ATP samples used were obtained from a previously prepared 100 mM ATP stock (Na-salt, Sigma-Aldrich). The standard calibration curves were obtained by adding 10 µl of ATP

solutions with concentrations ranging from 10^{-3} M to 10^{-7} M to wells in a dark 96 well plate containing 100 µl of luminescence reagent, as instructed by the manufacturer. The bioluminescence emitted was detected, after 5 minutes incubation at room temperature, using the Synergy 2 Multi-Mode Microplate Reader (BioTek). Standard calibration curves were obtained for every new experiment with the same buffer as in the tested samples.

The validation experiments were performed using a fixed ATP concentration of 10^{-5} M (10 times diluted after addition of the luminescence reagent). To test chemical denaturing conditions, ATP solutions were incubated with different denaturants on ice for a period of 30 minutes. To test physical denaturing conditions, ATP solutions were incubated at 95ºC for 10 minutes. Following the denaturing periods, ATP quantification was performed for each solution as described above. KCl titration solutions did not require any incubation period. All the validation experiments, as some other experiments in this project, were performed only once.

To determine the amount of ligand associated with the protein, ATP and AMP-eluted KtrA solutions were purified by size-exclusion chromatography and either stored at -20ºC or submitted to extensive dialysis. After the extensive dialysis period, both non-dialysed (T0) and dialysed solutions were denatured by boiling at 95ºC for 5 minutes. Following a 10 minutes spin at 12 000xg, 10 µl of each solution was processed as described above.

2.4. Protein quantification

Three different protein quantification techniques were used during this project.

2.4.1. Bio-Rad protein assay

20 µl of protein solution were added to 980 µl of Bio-Rad protein assay reagent (4 times diluted in double deionized water) and absorbance was measured at 595 nm wavelength in a spectrophotometer.Protein dilutions were made to restrict absorbance values between 0.1 and 1.0. Blank was set by adding 20 µl of buffer without protein instead of protein solution.

2.4.2. Direct Detect

Protein concentration was measured using the Direct Detect Spectometer (Merck Millipore). 2 µl of protein solution were analysed by spotting on a Direct Detect Assay-free Card. A typical result is shown in Appendix A.3.

2.4.3. Spectrometry

KtrA solution was appropriately diluted and absorbance at 280 nm wavelength was determined. The extinction coefficient, ε, 16 410 $cm^{-1}M^{-1}$ was used to determine the protein concentration according to the Beer-Lambert equation (1) [29].

$$Abs_{280} = \varepsilon lc \quad (1)$$

where Abs_{280} corresponds to the measured absorbance value, l corresponds to the length of the cuvette (generally 1 cm) and c represents the protein concentration.

ATP concentration was also determined using the Beer-Lambert equation, at 259 nm wavelength, with a ε value of 15.4 $cm^{-1}mM^{-1}$ [30].

2.5. Isothermal Titration Calorimetry

The ITC technique allows the measurement of the binding properties between a pair of molecules, for instance protein-ligand [31]. The MicroCal VP-ITC System (GE Healthcare) instrument possesses two distinct cells: a reference cell, where a blank solution is inserted (usually water), and a sample cell, containing the protein solution. The ITC technique is based on the measurement of the heat change that occurs upon the binding of the ligand to the protein in solution. This heat change is quantifyied from the power used by the instrument to compensate for the temperature difference between the reference and sample cells resultant from the heat release or absorbed [31]. Heat changes are recorded for each ligand injection into the sample cell. In my experiments, the ITC reference cell was filled with filtered double deionized water. Extensively dialysed KtrA (eluted from the ADP-agarose beads with AMP) was added to the sample cell at a concentration of 30 μM in a total volume of 2.5 ml. The ligands ATP, ADP or AMP, used as titrants, were diluted in filtered dialysis buffer to a concentration of 300 μM, ten times higher than the protein concentration. 284 μl of titrant were placed in the syringe and 47 injections of 6 μl each, spaced by 220 seconds, were made. Most experiments were run at 25^{o}C; experiments where the protein and titrant were dissolved with HEPES-containing buffer were run at 15^{o}C. The baseline power differential, DP, was set to 15 μcal/sec.

2.6. Molecular cloning

The mutants used in this project were obtained by common molecular biology techniques. Below, these techniques are described for one of the mutants I78V.

2.6.1. Oligonucleotide primers

A pair of oligonucleotide primers was designed for each mutant. The primers are sequences of wild type DNA with only a codon altered in the desired site of mutation. The pair of oligonucleotide primers designed to generate the I78V mutation was the following: 5'-TTGAATATGTGATTGTTGCC**G**TCGGAGCAAATATTCAAGCG-3' for the forward primer; 5'-CGCTTGAATATTTGCTCCGA**C**GGCAACAATCACATATTCAA-3' for the reverse primer. In bold are the bases altered in order to change the isoleucine codon to a valine codon.

2.6.2. PCR - Amplification of plasmid with mutant variation

A PCR reaction was performed using both the 2 oligonucleotide primers and the WT plasmid pET24dKtrA together with the high-fidelity Pfu DNA Polymerase (Thermo Scientific) according to the following reaction mixture:

Table 1 - Amplification reaction mixture

	Concentration	Volume (µl)	Company
Pfu buffer	10x	5.0	Thermo Scientific
dNTP	10 mM	1.0	Thermo Scientific
5'- primer	10 mM	1.0	Sigma-Aldrich
3'- primer	10 mM	1.0	Sigma-Aldrich
DNA template	10 ng/µl	3.0	-
DMSO	100%	2.5	Sigma-Aldrich
Pfu turbo	2.5 U/µl	1.0	Thermo Scientific
ddH_2O	-	35.5	-

The PCR reaction was performed using the T100TM Thermal Cycler (Bio Rad) and according to the following reaction cycle:

Table 2 - PCR cycle

		Temperature (ºC)	Time
1	Polymerase activation	95	4 min
2	Denaturing	95	1 min
3	Annealing	55	1 min
4	Extension	68	2 min/kb
5	Repeat 2-4	-	17 x
6	Extension	68	10 min
7	Deactivation	10	∞

The solution containing the PCR products was submitted to a DNA digestion using the restriction enzyme DpnI (10 U/µl, Thermo Scientific), in order to only digest the original WT template. 1µl of the restriction enzyme was added and the reaction took place at 37ºC for 2 hours. Finally, the resultant plasmids (10 µl) were used to transform competent *E. coli* BL21 (DH5α) cells following the same transformation protocol as in 2.1.1.

2.6.3. DNA purification

Extraction of engineered plasmids from transformed bacteria was achieved using NZY Miniprep kit (NZYtech) according to manufacturer's instruction. This was done with bacterial liquid cultures grown at 37ºC overnight in 10 ml of LB broth supplemented with kanamycin at 50 µg/ml. Purified DNA was resuspended in autoclaved double deionized water. Absorbance values at 260 nm were used to determine DNA concentration as well as its purity (260 nm/280 nm ratio >1.8).

2.7. Small scale expression

This procedure is similar to the one described in 2.1. and was used for a preliminary characterization of mutant proteins. *E. coli* BL21 (DE3) were transformed and grown at 37ºC, this time in 50 ml flasks (KIMAX), in LB broth supplemented with kanamycin (50 µg/ml). When cultures reached an OD_{600nm} of 0.6, protein expression was induced by addition of IPTG (500 µM, NZYtech) and ethanol (2.0%) and incubation at 20ºC for ~14h-16h.

Induced cultures were centrifuged at 4ºC, for 10 minutes at 2 500xg with the resulting pellet being resuspended in Lysis Buffer supplemented with the protease inhibitors Leupeptin (1 µg/ml), Pepstatin (1 µg/ml) and PMSF (1 mM). Cells were lysed by sonication using the Sonifier (Branson) with a total lysis time of 6 minutes (with cycles on/off of 10s/20s), and an output set for 5 and on cycles of 50%. 1 ml of the each resulting solution was centrifuged for

10 minutes at 12 000xg. The supernatant and pellet were separated and the latter resuspended in 1 ml of Lysis Buffer. 20 µl of each was run in a 15% SDS-PAGE gel and protein bands stained with Coomassie Blue dye.

The protein containing supernatants were incubated with ADP-agarose resin overnight at 4ºC. Protein was, then, eluted using 1 mM ATP or ADP solutions or a 50 mM AMP solution. 10 µl of the eluted solutions, and 8 µl of beads were run in a 15% SDS-PAGE gel and protein bands were, once again, stained using Coomassie Blue dye.

2.8. Tryptophan fluorescence

500 ng of extensively dialysed KtrA mutants were supplemented with 100 µM of ATP or ADP. Non supplemented protein solutions were also used. Tryptophan fluorescence of WT protein and mutants R16A, R16K and E125Q was detected using the FluoroMax-4 Spectrophotometer (Horiba). Samples were excited with 290 nm radiation and emitted fluorescence was detected within the range 310-450 nm. Triplicates were executed.

2.9. Protein crystallography

Purified AMP-eluted KtrA was concentrated using a Vivaspin 6 Centrifugal Concentrator (Vivaproducts). Crystal formation by using the sitting drop technique was screened using the commercial screening conditions Morpheus HT-96 1 and 2 (Molecular Dimensions), Wizard Classic 1 and 2 (Rigaku) and NeXtal (QIAGEN) as well as the manually developed crystallization condition:

- Tris-HCl (100 mM, pH 8.5)
- Allyl Methil Sulfide, AMS (2.2 M)
- Glycerol (10%)

A sub-screening of conditions that succeeded in originating crystals using commercial additives (Additive Screen, Hampton Research) was made.

Diffraction data was collected at the Soleil synchrotron.

2.10. Statistical analysis and Software

Statistical analysis was performed using GraphPad Prism 6 software. PyMOL software was used to analyse the structure of KtrA. ITC data were treated and analysed using the Origin7 software (OriginLab). Origin7 software was also used, alongside FluorEssence (Horiba) in the processing of Tryptophan Fluorescence data.

Chapter 3

Results

The principal objective of this project is to determine the binding properties of both ATP and ADP to the cytosolic regulatory protein of the KtrAB complex, KtrA. The correct determination of these properties requires the complete removal of ligands from the KtrA binding pocket. Here, a method is proposed by which the binding pocket becomes ligand-free while the protein remains stable in solution. In such conditions, the determined dissociation constant, K_D, for the binding of the small ligands AMP, ADP and ATP to the wild type KtrA were 4 μM, 763 nM and 690 nM, respectively. At the same time, a set of mutant proteins were developed by changing key binding-site residues with two objectives: find a stable mutant with lower ligand affinity and understand the role played by these residues in the stability and conformation of KtrA. These mutants were partially characterized and their behaviour when binding to ATP and ADP was compared to the wild type protein.

3.1. Ligand removal

This project's first step consisted in developing a way to completely remove any ligands from the KtrA binding pocket without destabilizing the protein in solution.

Purified KtrA stability is only maintained when a ligand is bound [personal communication]. This fact, allied to the high cytosolic concentration of ATP in *E. coli*, 9.6 mM [26] and the high affinity of KtrA to ATP [19, 20], results in the preparation of KtrA that retains ATP after purification. Furthermore, as one can see in the Materials and Methods chapter, the purification of KtrA requires an elution step, where the protein is eluted with a solution containing high-concentrated ATP, ADP or AMP. Although the excess of ligand in solution is removed during size-exclusion chromatography, some of it is likely to remain bound to the protein. This preparation is therefore not ideal for determining the ligand binding properties of KtrA.

An efficient way of removing a small ligand from a protein solution is through dialysis in a ligand-free buffer. Such buffer needs to ensure the stability of the protein. Previous attempts

in the lab to remove ligands associated with KtrA have not been successful: either the procedure failed to completely remove the ligands, or the protein was destabilized and precipitated.

I started my project by testing four different dialysis buffers for compatibility with KtrA purified in the presence of AMP (table 3).

Table 3- Dialysis Buffers

Buffer D1 • 50 mM Tris-HCl (pH 7.5) • 150 mM KCl • 5 mM DTT • 1 mM Adenine	Buffer D2 • 50 mM Tris-HCl (pH 7.5) • 150 mM KCl • 5 mM DTT • 10 mM Adenine
Buffer D3 • 25 mM K^+ PO_4^{3-} (pH 8.0) • 100 mM KCl • 1 mM TCEP	Buffer D4 • 150 mM K^+ PO_4^{3-} (pH 8.0) • 5 mM DTT

In D1 and D2 buffers, Tris-HCl was used to buffer the solution at a pH around 7.5; KCl was used to try to stabilize KtrA (K^+ ion serves this purpose) since some intracellular proteins are sensitive to the presence of Na^+; DTT is a reducing agent, which prevents intra and intermolecular disulphide bonds between cysteine residues, hindering the formation of protein aggregates; and adenine served as a potential low-affinity substitute of the removed ligand, stabilizing the binding pocket. As for the remaining two buffers, the phosphate (PO_4^{3-}) component serves both as buffer, keeping the pH ~8.0, and binding site stabilizer since it may be a substitute for the phosphate groups of ATP or ADP; the K^+ ion has the same role mentioned above, as well as TCEP (a reducing agent) or DTT, acting both as reducing agents.

The protein in solution was recovered after three days of dialysis and some of its characteristics were evaluated. Buffers D1 and D3 are not compatible with KtrA since the majority of the protein destabilizes and precipitates: 53.49% and 87.73% of protein is lost, respectively (table 4). The amount of stable KtrA is higher for D2 and D4 buffers, with the latter having the smaller rate of precipitated protein (5.95% against 19.90% for D2).

The size-exclusion chromatography profiles corresponding to each buffer are represented in figure 5. Peaks around 8 ml correspond to protein aggregates and octameric KtrA elutes at 12.5 ml. Adenine elutes at 27 ml and ATP, ADP and AMP elute around 20 ml. Most of the soluble protein in D1 and D3 buffers is aggregated. D2 buffer still has some aggregation present and D4 buffer prevents this destabilizing event. Based on these observations, D4 buffer is the most suitable buffer for KtrA dialysis.

Table 4 - Percentage of precipitated KtrA after three days dialysis with four different dialysis buffers

Buffer	Before Dialysis (mg)	After Dialysis (mg)	Protein lost (%)
D1	4.644	2.16	53.49
D2	4.644	3.72	19.90
D3	4.644	0.57	87.73
D4	1.783	1.677	5.95

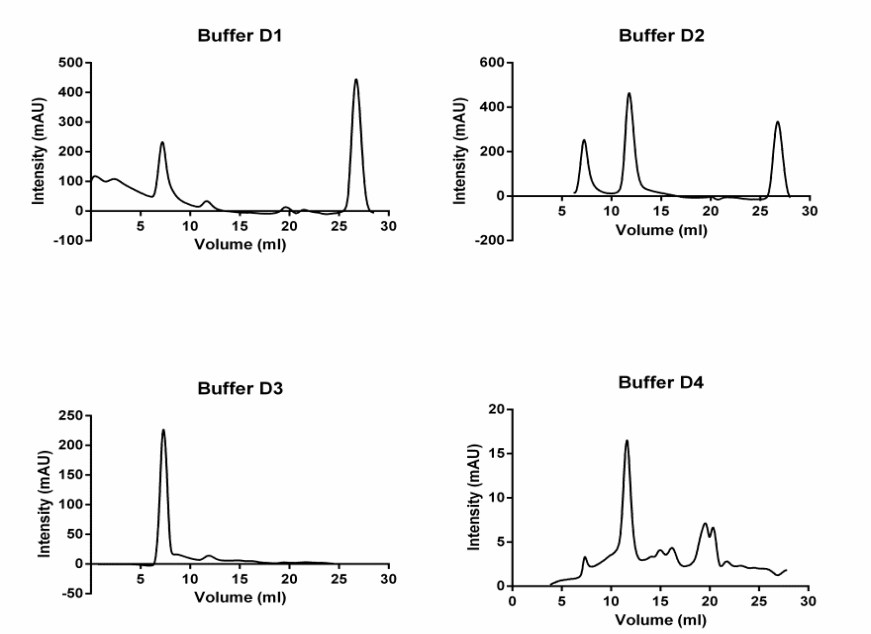

Figure 5 - Size-exclusion chromatography profile for KtrA dialysed over three days with four different buffers: D1; D2; D3 and D4 (see table 3).

3.1.1. ATP quantification

Understanding the extent of ligand removal after dialysis becomes possible by accurately quantifying the ATP associated with protein. One way to do so is by measuring the luminescence intensity resultant from the reaction (2) catalysed by recombinant luciferase, in which the ATP is the limiting component, using the ENLITEN ATP assay (Promega).

$$ATP + Luciferin + O_2 \rightarrow Oxylucifer\,in + AMP + PPi + CO_2 + Light \quad (2)$$

The utilization of this assay is dependent of previous validation for critical conditions. First of all, a standard calibration curve was obtained (figure 6) and the optimal ATP range was defined to be from 0.1 pmol to 10 000 pmol of ATP. I also noted that there was a significant variation in the values of the standard curve between different experiments and therefore new curves were determined for every assay.

It has been reported that the reaction catalysed by the luciferase is affected by high salt concentrations [32]. Since the stability of KtrA in solution is ensured by the presence of salt, usually KCl, I needed to evaluate whether the salt concentrations used for preparation of KtrA interfered with the luciferase assay. A titration was performed using increasing KCl

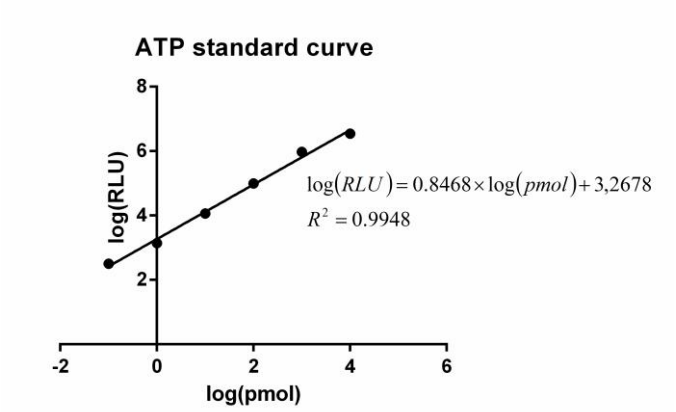

Figure 6 - Example of ATP standard calibration curve. Logarithmic curve with the amount of ATP represented in the xx axis [log (pmol)] and the Relative Light Units in the yy axis [log (RLU)].

concentrations with a fixed amount of ATP (100 pmol) (figure 7). Although there is a decrease in the luminescence signal, its extent is not limiting and concentrations up to 150 mM of K^+ containing solutions were used.

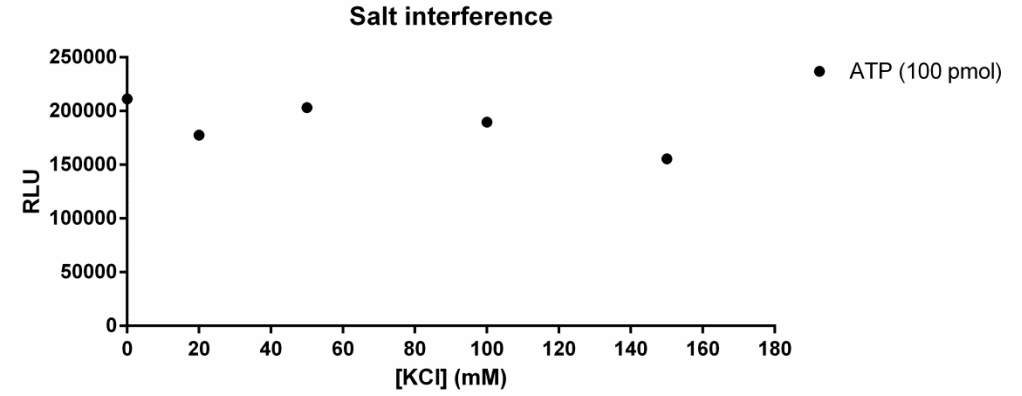

Figure 7 - Luminescence intensity of a fixed ATP amount (100 pmol) in solutions with crescent KCl concentrations.

Another aspect likely to influence the luminescence intensity is the denaturing condition used to free into solution the bound ligand. This time, both salt concentration and ATP amount were fixed at 150 mM and 100 pmol, respectively, and four different denaturing conditions were assessed (figure 8). Both guanidine hydrochloride (3M) and TCA (2.5%) lowered drastically the luminescence signal. The urea (4M) solution reduced the signal as well, though not as radically, while boiling the ATP solution did not affect the intensity of the signal. Denaturation by boiling the protein sample was the method chosen for the quantification assays.

For the ATP quantification assay, purified KtrA was eluted using either ATP or AMP. The protein solutions were submitted to an extensive dialysis in D4 buffer, with four buffer changes over, at least, four days. Both dialysed and non-dialysed (T0) protein solutions were tested. Protein samples, in a 150 mM salt solution, were denatured by boiling for 5 minutes at 95°C. The results show that, at T0, the ATP eluted protein solution has 1.4 (± 0.2) moles of ATP per mole of protein (figure 9). This indicates that a high concentration of ligand remains in solution after protein purification by size-exclusion chromatography. After an extensive dialysis using the D4 dialysis buffer, there is a significant drop in the molar ratio to 0.0011 (± 0.0015) mole of ATP per KtrA mole. This data confirms the successful removal of ATP during

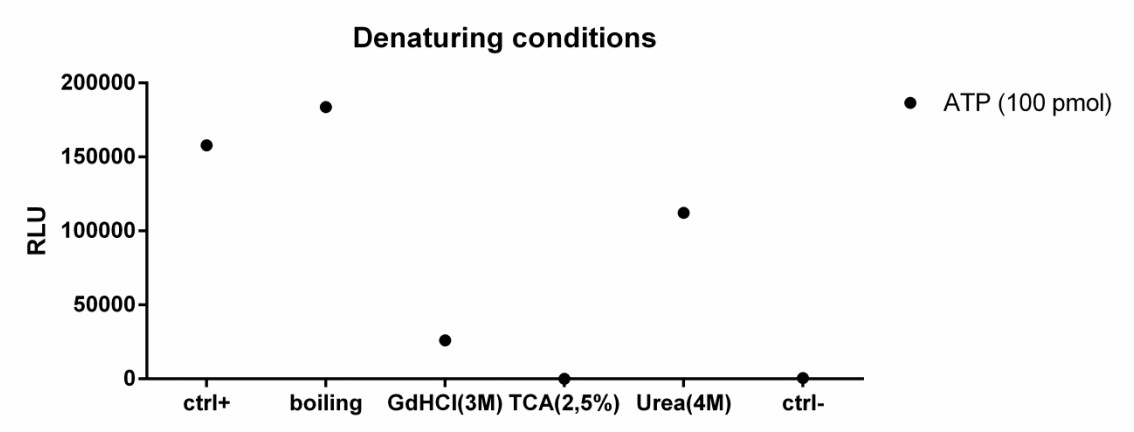

Figure 8 – Effect of four different denaturing conditions in quantification of ATP by luciferase assay. For ctrl + an untreated ATP solution (100 pmol) was used and for ctrl – an ATP-free solution was used.

extensive dialysis in D4 dialysis buffer. For the AMP eluted protein, the ATP signal is low in both non-dialysed and dialysed KtrA, with ATP:KtrA ratios (mol:mol) of 0.0036 (± 0.0015) and 0.010 (± 0.0082), respectively, demonstrating that elution of KtrA from ADP-agarose beads with AMP is sufficient to remove most of the ATP associated with KtrA. Elution of KtrA using AMP followed by extensive dialysis was the chosen methodology to ensure most of the ligand is removed.

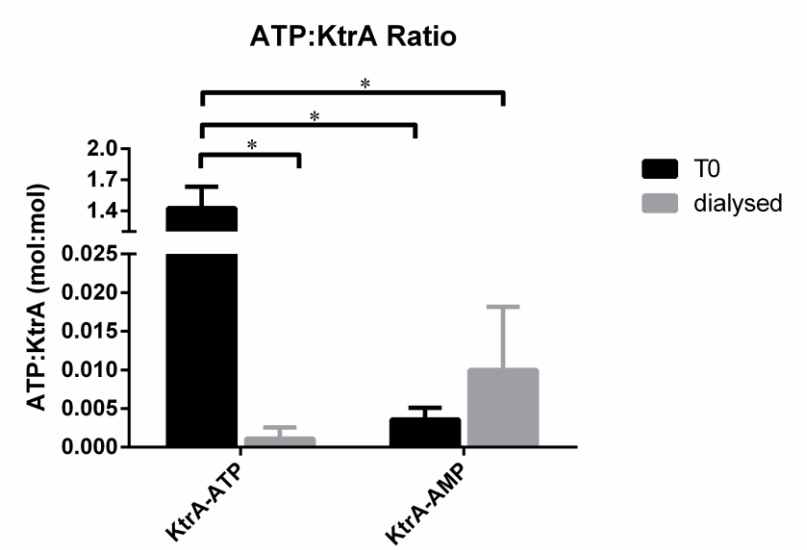

Figure 9 – ATP:KtrA molar ratio after ATP quantification in KtrA samples. Non-dialysed (black, T0) and extensively dialysed (grey) samples of ATP (left) and AMP (right) eluted KtrA were tested. For better resolution, the yy axis was broken at 0.025 and resumed at 1.2. The mean values represented are 1.4272 and 0.0011 mol:mol for KtrA-ATP T0 and dialysed, respectively, and 0.004 and 0.010 mol:mol for KtrA-AMP T0 and dialysed. * marks statistical significance between referred data with $p<0.0001$.

3.2. KtrA binding properties

The characterization of the KtrA ligand binding properties was performed using the ligand-free KtrA prepared by the methods outlined above. In particular, I used Isothermal Titration Calorimetry (ITC) to determine the binding affinities of ATP, ADP and AMP to KtrA. A factor to take in account is that reducing agents' oxidation may influence the ITC background signal [33]. Given that, DTT was removed from the D4 dialysis buffer in the last buffer change. Figure 10 represents both raw and treated ITC data obtained after titrating ligand-free KtrA with ATP, ADP or AMP. From this data it was possible to determine ligand affinity,

stoichiometry and enthalpy of binding reaction. AMP is the ligand with lower affinity, having a K_D of 4μM, while ATP and ADP have the same affinity (ATP K_D 690nM and ADP K_D 763nM).

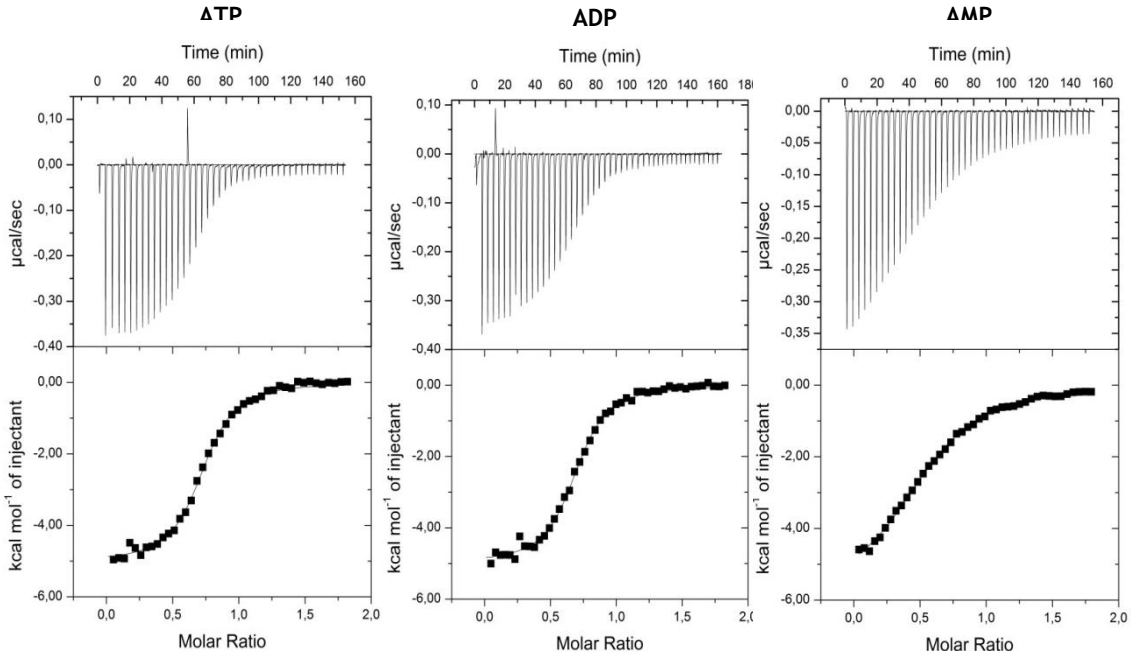

N = 0.727 binding sites	N = 0.694 binding sites	N = 0.569 binding sites
K_D = 689.66 nM	K_D = 763.36 nM	K_D = 4.082 μM
ΔH = -5024 cal/mol	ΔH = -4987 cal/mol	ΔH = -5831 cal/mol

Figure 10 - ITC data for extensively dialysed KtrA in D4 dialysis buffer without DTT. ATP, ADP and AMP were used as titrants and the respective graphs are represented from left to right. At the top of each graph is shown the raw ITC data and at the bottom the processed ITC curves. The binding sites per KtrA molecule, N, dissociation constants K_D, and enthalpy, ΔH, values are shown below the graphs.

3.3. Characterization of KtrA mutants

The determination of the structure of KtrA bound to ATP and ADP has led to the identification of the residues that constitute the ligand binding pocket. With the objective of understanding their role in KtrA stability, conformation and binding affinity of ATP and ADP, some of these residues were mutated. Furthermore, if stable mutants with lower affinity for ATP or ADP could be found, they could be used in biochemical and cell-based experiments to probe the properties of the KtrAB complex.

After careful analysis of the KtrA structure, three binding pocket residues that are likely involved in ligand binding were chosen to produce four mutant proteins. The objective was to assess the importance of these residues in the binding of KtrA to its ligands. The mutants produced were D36N, D36T, I37T and I78V. The residues are shown in figure 11.

First, I analysed how these mutations affected the protein expression level. Bacteria were collected before (T_0) and after protein expression induction (T_{ON}) and protein expression was analysed (figures 12a and 12b). Although all the mutants are expressed, the levels of D36N and D36T are much lower compared to the wild type protein, indicating that a mutation in

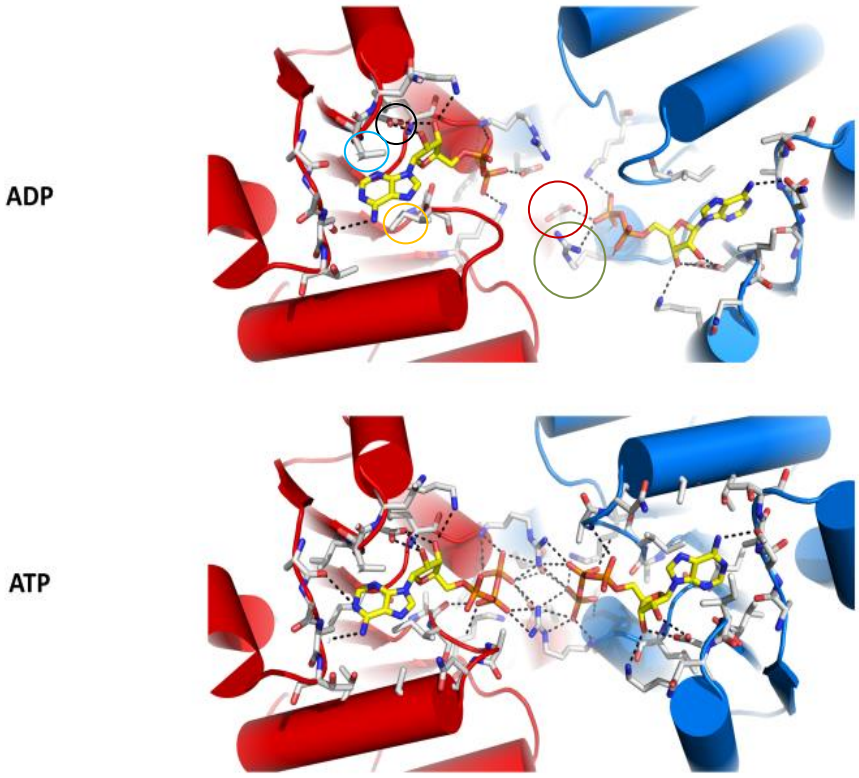

Figure 11 - Close up of a KtrA dimer's binding sites upon binding of ADP (top) or ATP (bottom). The mutated binding site residues described in this project are highlighted in the top figure. The aspartic acid (D) in position 36 is circled in black; the isoleucines (I) in positions 37 and 78 in blue and orange, respectively; the arginine (R) in position 16 is circled in green; and the glutamic acid (E) in position 125 in red. A contraction of the dimer is visible upon binding of ATP, mediated by the interaction of this molecule with both the highlighted residues.

position 36 hinders protein expression. The expression levels of the other two mutants do not seem to differ from the wild type.

After cell lysis, both soluble and pellet fractions were visualized in order to assess how protein's solubility is affected by the mutations. A destabilization of the protein is detected for mutants D36N and D36T since no protein is present in the soluble fraction, indicating a loss of solubility (figure 12b). Due to this low solubility, purification of these mutants was not pursued. Both I37T and I78V mutant proteins are detected in the soluble fraction, similarly to the wild type protein, indicating that these mutations do not interfere with the protein's solubility (figure 12c).

The soluble mutants were then incubated with ADP-agarose beads and eluted with ADP and ATP afterwards. The I78V mutant did not bind to the ADP in the beads which could mean that its affinity for ADP has been greatly affected. On the other hand, the I37T mutant was bound to the beads and eluted by both ligands, similarly to the wild type protein (figure 12d).

Other four interesting mutant proteins, already existent in the lab, were also characterized. These mutants originated from the substitution of two key residues likely involved in the conformational changes mediated by ligand binding. The arginine in position 16 interacts simultaneously with the phosphates of the two ATP molecules bound to a KtrA dimer (figure 11). This interaction is not detected when ADP is bound due to the lack of the γ-phosphate group. The glutamic acid in position 125 also participates in the coordination of

the protein conformation by interacting with the ligand phosphate groups (figure 11). The four mutants created were R16A, R16K, E125A and E125Q.

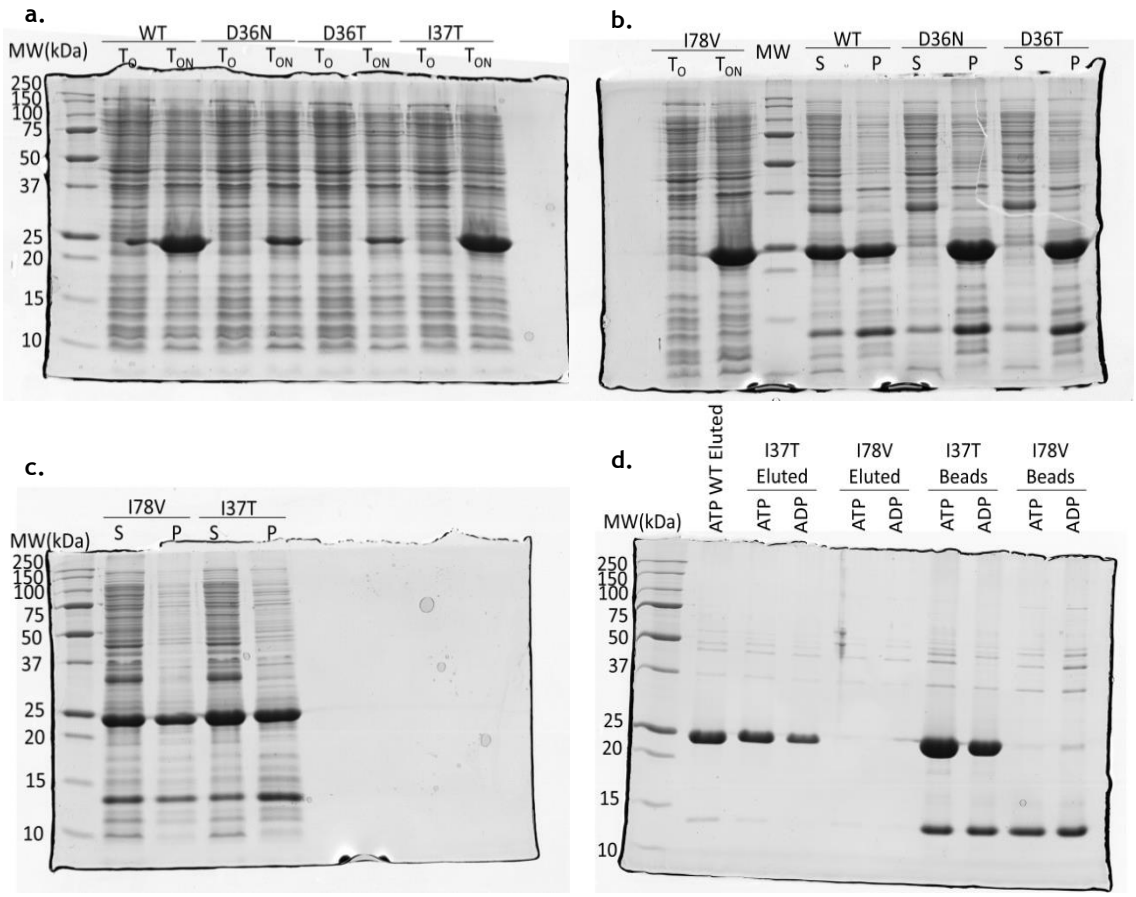

Figure 12 - SDS-PAGE gels, showing purification steps for the KtrA mutants D36N, D36T, I37T and I78V as well as the wild type (WT) protein. (a) overnight induction of protein expression in *E. coli* strain BL21(DE3). T0: before induction; T_{ON}: after induction. (b) overnight induction of I78V mutant and solubility assessment of WT, D36N and D36T mutants, after cell lysis. S: soluble fraction; P: pellet. (c) Distribution of I37T and I78V mutants between soluble and insoluble fractions of cell lysate. (d) WT KtrA and I37T and I78V mutants eluted with either ATP or ADP – first five wells (after MW) – or still bound to ADP-agarose beads – last four wells.

These four mutants expressed well and were found in the soluble fraction of lysed cells, confirming the maintenance of the protein's solubility (figures 13a and 13b). With the exception of E125A that did not bind to ADP-agarose beads, the other three mutants were successfully bound to the beads and eluted with an AMP solution (figures 13c and 13d). Note that E125A was present in the cell lysate as shown in figure 13d.

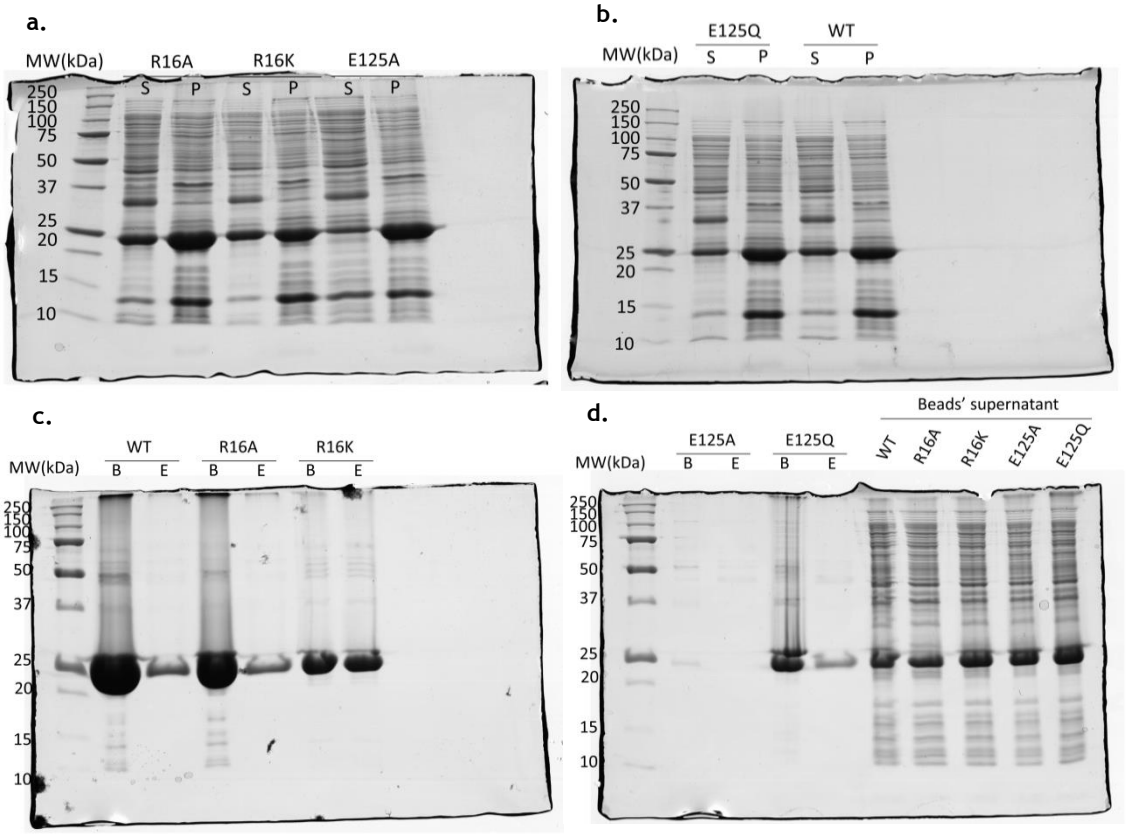

Figure 13 - SDS-PAGE gels, showing purification steps of the KtrA mutants R16A, R16K, E125A and E125Q as well as WT protein. (a) Distribution of mutants R16A, R16K and E125A in fractions of cell lysate. S: soluble fraction; P: pellet. (b) Distribution of E125Q mutant and WT protein in cell lysate fractions. (c) elution of R16A and R16K mutants, as well as WT protein, with an AMP solution, from ADP-agarose beads. B: fraction still bound to beads; E: eluted fraction. (d) elution of mutants E125A and E125Q, with an AMP solution, from ADP-agarose beads and supernatant resultant from incubation with the beads.

3.3.1. Tryptophan fluorescence

A previous observation made in the lab reported that ATP binding to KtrA results in a change in tryptophan fluorescence which does not occur when ADP is used as titrant (figure 14a). Such alteration in fluorescence is likely the result of the conformational change induced by ATP binding [6]. Since the mutations reported here correspond to binding-site residues, it becomes interesting to understand if tryptophan fluorescence changes as observed for the wild type protein.

These experiments were performed after AMP removal by extensive dialysis in D4 dialysis buffer. In table 5 are shown the values of the relative difference between the fluorescence intensity measured for ligand-free protein and ATP or ADP-bound protein. These values were obtained from spectra similar to the example shown in figure 14a. In figure 14b there is a graph depicting the values in table 5. The previously made observation of a significant fluorescence intensity decrease with ATP binding in the wild type protein and little or no change with ADP binding was confirmed. In contrast, none of the three mutants tested showed a significant difference between the tryptophan fluorescence of the ATP and the ADP bound-states. Curiously, for the R16K mutant, the binding of ATP and ADP led to a dramatic increase in fluorescence intensity. The high error bars obtained suggest high variation among different experiments. The assay should be repeated to produce more reliable results.

Table 5 - Relative difference to ligand-free KtrA, in percentage, of tryptophan fluorescence intensity in ATP or ADP-bound protein. The bottom lines represent the mean and the standard deviation values.

	WT		R16A		R16K		E125Q	
	ATP	ADP	ATP	ADP	ATP	ADP	ATP	ADP
(%)	17.48	10.17	12.02	3.53	-37.25	-41.60	-3.27	-7.29
	24.14	12.71	16.06	18.84	-18.42	-7.10	1.48	9.48
	26.19	-0.13	16.44	14.41	-12.68	-6.89	13.79	6.05
Mean	22.60	7.58	14.84	12.26	-22.79	-18.53	4.00	2.75
Std dev	5	7	2	8	13	20	9	9

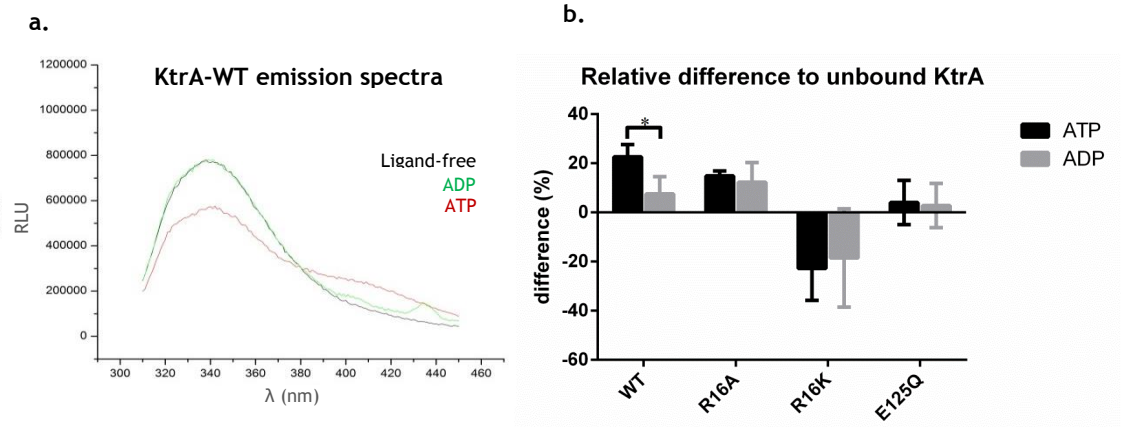

Figure 14 - Tryptophan fluorescence. (a) wild type KtrA emission spectra upon excitation at 290 nm. Represented in black is the unbound wild type protein emission spectrum, while the ATP and ADP-bound protein are in red and green, respectively. (b) Relative difference to ligand-free protein. Bars in black correspond to the relative difference verified upon ATP binding while grey bars relate to ADP binding.
* marks statistical significance between referred data with $p<0.05$.

3.3.2. Determination of mutant binding energetics - ITC

Assessing the binding affinities of the mutant proteins to ATP and ADP and comparing them to the wild type KtrA could give some insight regarding the role of the mutated residues in ligand binding.

The mutants R16A and R16K were treated in a similar way as the wild type protein in 3.2. and the resultant ITC data is presented in figure 15.

The ATP K_D values for R16K and R16A mutants (725 nM and 769 nM, respectively) are similar to each other and similar to the K_D determined for the WT protein. On the other hand, titration with ADP revealed a slightly lower affinity of both mutants to ADP, when compared to the WT protein, with K_D values of 1.55 μM and 1.22 μM, respectively.

The N values determined for these mutants are unexpectedly low when compared to the expected 1 binding site per KtrA molecule. There are two possible explanations for this observation: 1) the ligand or protein concentrations were not correctly determined; 2) only a fraction of the protein is competent for ligand binding. The first hypothesis was rejected after repeating the titration with ligand and protein concentrations that were verified by multiple methods. If the second hypothesis is correct, it raises the idea that the extensive dialysis affected the stability of KtrA. In order to understand how the dialysis buffer used

could be interfering with the determination of the binding properties, further studies will have to be conducted. For instance, the assessment of the melting temperature of the protein after extensive dialysis in D4 buffer would indicate a disturbance in the protein stability if a lowering in this parameter was observed when compared to the protein purified by size exclusion chromatography.

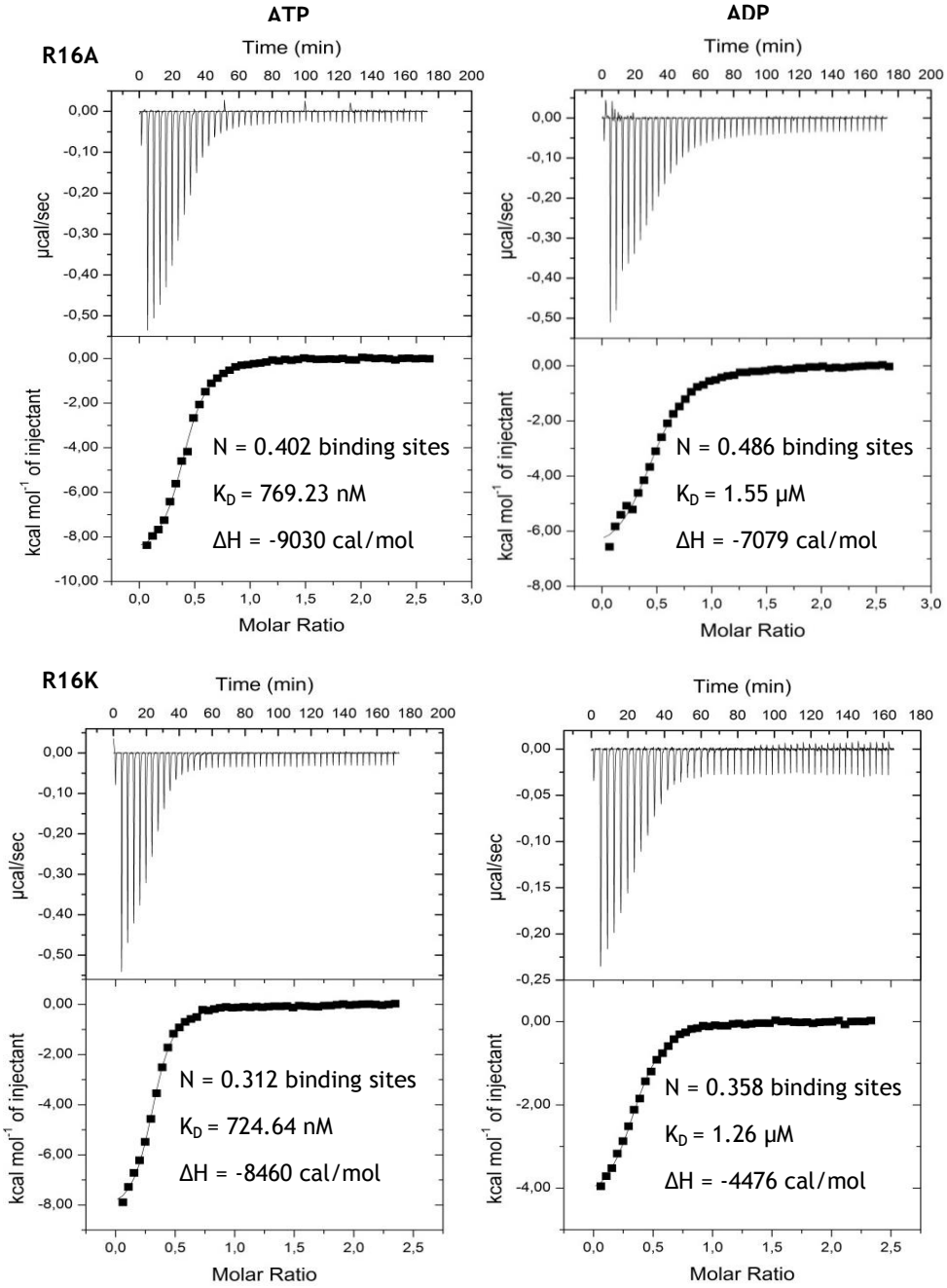

Figure 15- ITC data for extensively dialysed KtrA mutants R16A (top) and R16K (bottom) in D4 dialysis buffer without DTT. ATP (left) and ADP (right) were used as titrants. At the top of each graph is shown the raw ITC data and at the bottom the processed ITC curves. The binding sites per KtrA molecule, N, dissociation constants K_D, and enthalpy, ΔH, values are shown inside the graphs.

As an alternative, the protein was prepared in the presence of AMP which has lower affinity for KtrA than ADP or ATP. The ITC titrations were repeated also in the presence of AMP, in a buffer composed of HEPES, pH 7.5 (50 mM), TCEP (1 mM), KCl (150 mM) and AMP (50 µM). Since TCEP does not interfere greatly with the ITC signal, I decided to include it in

the buffer to promote protein stability. These competition experiments were also conducted at 15ºC instead of the 25ºC used in the previous experiments.

The competition titrations performed for the R16A mutant (figure 16) are fairly complex since they could only be fitted with a model that included 4 sequential binding sites. The titration using ATP results in the 4 distinct binding sites with K_D values of 10.27 µM; 12.15 µM; 9.26 µM and 9.71 µM. These results suggest the existence of binding dependency between the octamer composing binding sites: The binding of an ATP molecule to one binding site will influence the affinity of the subsequent binding sites. The ADP titration data has a lower signal but it can also be fitted with a 4 sequential binding sites model, presenting K_D values similar to the ones observed for ATP titration: 11.26 µM; 18.05 µM; 4.07 µM; and 12.33 µM.

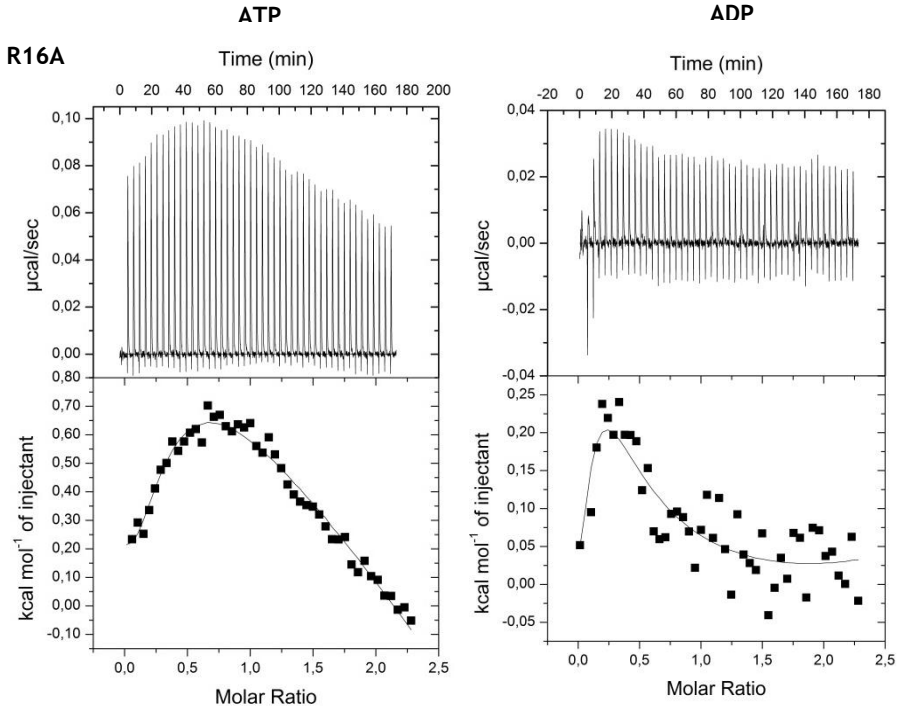

N = 4 binding sites	N = 4 binding sites
K_{D1} = 10.27 µM K_{D2} = 12.15 µM	K_{D1} = 11.26 µM K_{D2} = 18.05 µM
K_{D3} = 9.26 µM K_{D4} = 9.71 µM	K_{D3} = 4.07 µM K_{D4} = 12.33 µM
ΔH_1 = 294.2 cal/mol ΔH_2 = 33.14 cal/mol	ΔH_1 = 50.90 cal/mol ΔH_2 = 3133 cal/mol
ΔH_3 = 9403 cal/mol ΔH_4 = -15450 cal/mol	ΔH_3 = -4954 cal/mol ΔH_4 = 3179 cal/mol

Figure 16- ITC data for KtrA mutant R16A saturated with 50 µM AMP, in HEPES buffer. ATP (left) and ADP (right) were used as titrants. . At the top of each graph is shown the raw ITC data and at the bottom the processed ITC curves. The binding sites per KtrA molecule, N, dissociation constants K_D, and enthalpy, ΔH, values are shown below the graphs.

In contrast, under similar conditions, the mutant R16K data is fitted with a single binding site model. Titration with ATP resulted in a surprisingly low K_D value of 111.23 nM and an N value of 0.949 binding sites per KtrA molecule. For ADP, the K_D value is 5.50 µM with an N value 0.965 binding sites per KtrA molecule (figure 17). Since these experiments reflect a competition with AMP for the binding sites of KtrA, the affinity measured should decrease. This tendency is, indeed observed upon titration with ADP but not with ATP. Note that the signal detected for ADP titration in both mutants is weaker than with ATP.

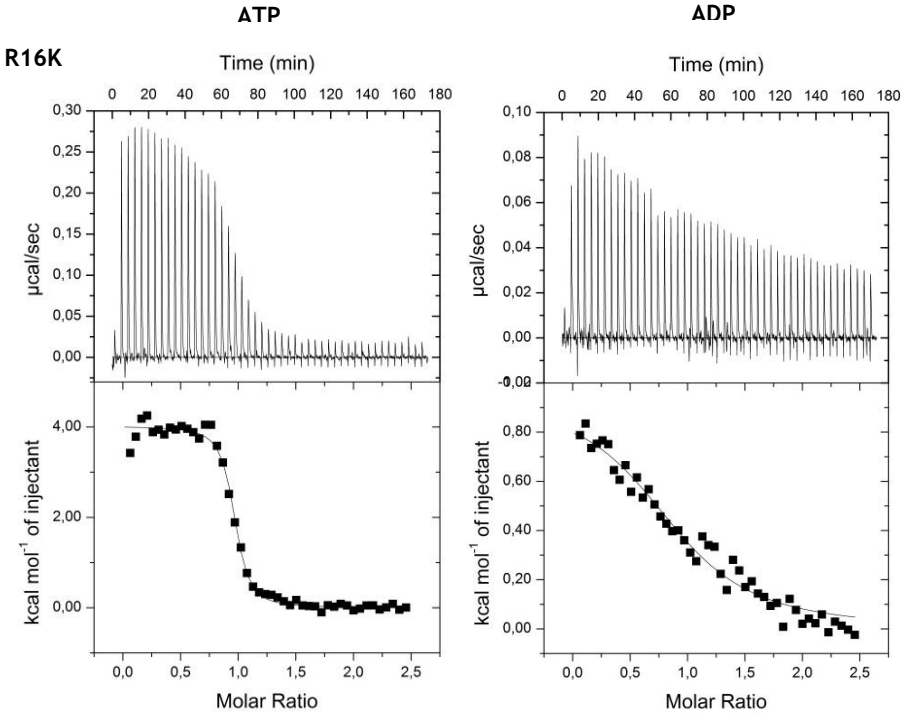

Figure 17 - ITC data for KtrA mutant R16K saturated with 50 µM AMP, in HEPES buffer. ATP (left) and ADP (right) were used as titrants. At the top of each graph is shown the raw ITC data and at the bottom the processed ITC curves. The binding sites per KtrA molecule, N, dissociation constants K_D, and enthalpy, ΔH, values are shown below the graphs.

3.4. AMP-bound KtrA crystallization

During this project, I also accomplished the crystallization of AMP-bound KtrA. Resolving the structure of the KtrA-AMP complex would define what is the conformation of KtrA when AMP is bound and what it compares with the conformations of KtrA bound to ATP and ADP [6]. AMP-eluted KtrA was purified using size-exclusion chromatography. After a screening using several crystallization conditions, the one that originated the most interesting crystals was the following:

- Tris-HCl (100 mM, pH8.5)
- Allyl Methil Sulfide, AMS (2.2 M)
- Glycerol (10%)

The crystals formed were improved by adding the additives $LiCl_2$ (figure 18a) or Phenol (figure 18b).

However, the diffraction data collected at the synchrotron only extended to ~5Å. At this resolution it is not possible to define the structural details of the protein structure. Further improvement of quality of the crystals is necessary.

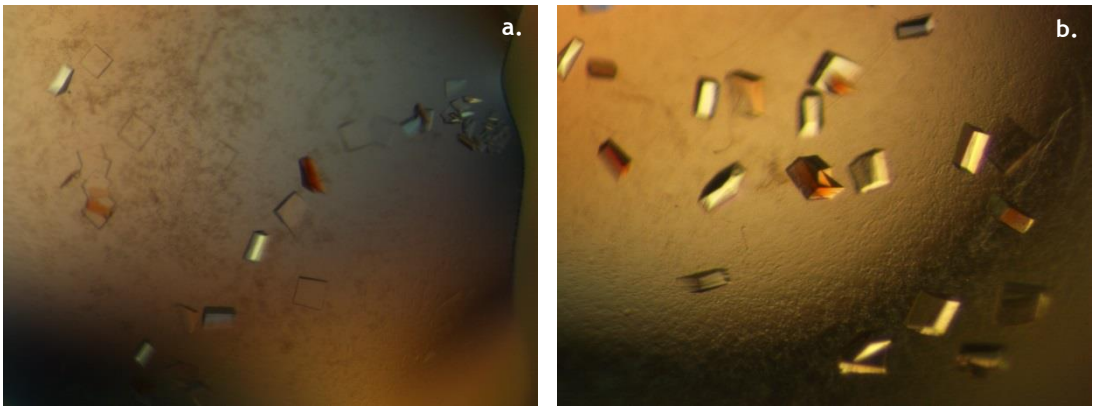

Figure 18 – Amplification showing the crystals obtained for AMP-eluted KtrA protein using the described condition, supplemented with (a) $LiCl_2$ and (b) Phenol.

Chapter 4

Discussion

KtrAB regulation most likely involves a conformational change upon ligand binding to the cytosolic regulatory protein, KtrA [21]. Given their relative high affinity for KtrA [19, 20], ATP and ADP are presented as the possible main effectors behind KtrA conformation changes. This idea is supported by the resolved KtrA structure in which the alternate binding of ATP and ADP resulted in alterations in KtrA conformation [6].

However, the mechanism by which the binding of the referred ligands modulate the activation of KtrAB is still unknown. Determination of the binding properties of ATP and ADP to KtrA represents a crucial step towards the understanding of such mechanism. Although some groups have already tried to determine the K_D value for ATP-KtrA binding [19, 20], the discrepancy between the obtained values (600 nM and 9 μM) is too large to represent convincing results.

4.1. Ligand removal and KtrA binding properties assessment

One of the reasons why it has been difficult to determine the binding properties of KtrA relates to protein stability after purification. In fact, KtrA seems to be stable only in the presence of a ligand. The major problem associated with the constant presence of a high affinity ligand in the KtrA binding pocket is the impact that this condition has in the affinity experiments. The pre-existing ligand will compete with the titrant for the binding site, making it impossible to determine the real binding properties of the tested molecule to KtrA.

The most straightforward way of removing a small molecule bound to a protein binding site is by dialysing the protein solution. So far, this approach has not been very successful, due to the referred lack of stability of KtrA when a ligand is not present. Thus, when the protein solution is submitted to a short dialysis period the ligand is not completely removed, while long dialysis periods often resulted in aggregation of the protein [personal communication]. In this project I tested a set of different dialysis buffers for compatibility

with the protein solution. The extent of ligand removal after extensive dialysis was assessed using a luciferase-based assay. After proving the efficiency of the chosen dialysis method, the ATP, ADP and AMP binding properties to ligand-free KtrA were determined by ITC.

The more phosphate groups (PO_4^{3-}) the adenosine-containing ligands possess, the higher their relative affinity to KtrA binding sites seems to be [6]. It was reasoned that, since KtrA binds adenosine-containing ligands, the protein would be more stable in solution if adenine was included in the dialysis buffer. The expectedly low affinity to adenine would lead to a significant decrease in competition during affinity determination assays. Therefore, two adenine based buffers were tested as dialysis buffers. In addition, two buffers with different phosphate concentrations were also tested as possible dialysis buffers, given the potential of this group to stabilize KtrA.

For both adenine and phosphate based buffers, higher concentrations resulted in higher protein stability. In fact, the 10mM adenine D2 buffer and the 150mM phosphate D4 buffer led to low protein aggregation (only 19.90% and 5.95%), while the 1mM adenine D1 buffer and the 25mM phosphate D3 buffer caused the loss of 53.49% and 87.73% of protein, respectively. The D4 dialysis buffer was the one chosen for the following steps of this study. In order to ensure the removal of as much ligand as possible, KtrA was dialysed in D4 buffer for at least four days, with four buffer changes in between.

The efficacy of the extensive dialysis was assessed using the ATP quantification kit ENLITEN ATP quantification assay. One of the critical aspects to take into account in the use of this kit is high salt concentration [32]. Although inhibition is detected in figure 7, its extent was not considered to invalidate the use of the assay with KtrA. Only ATP free in solution is detected using the ENLITEN ATP quantification assay. Since the ligand is bound to KtrA, a previous protein denaturation step is required. After testing the effect of different denaturation processes in an ATP solution, it was found that the chemical processes altered the reaction. On the other hand, boiling, a physical protein denaturation process, did not affect the luminescence signal and therefore this method was used in the following steps.

Before dialysis (T0), the molar ratio ATP:KtrA (mol:mol) is 1.4 (± 0.2), which indicates that the KtrA binding sites are fully occupied even after its passing through a size-exclusion chromatography column. In contrast, after extensive dialysis, the molar ratio drops to 0.0011 (±0.0015). This residual value confirms the removal of ATP from the KtrA binding pocket after an extensive dialysis in D4 buffer. AMP-eluted KtrA was also submitted to the ATP-specific ENLITEN ATP quantification assay. No ATP was detected in this sample, both before and after extensive dialysis. The ATP quantification assays clearly confirm the efficacy of D4 dialysis buffer, as well as of the elution with AMP from the affinity column, in the removal of ATP from KtrA.

The three main parameters determined during ITC experiments are the N value, which indicates the stoichiometry of binding; the dissociation constant, K_D; and the enthalpy variation, ΔH.

The binding properties of KtrA after extensive dialysis and titration with ATP, ADP and AMP were the K_D values 689.66 nM, 763.36 nM and 4.082 µM, respectively and the N values

0.727, 0.694 and 0.569. This shows that KtrA binds ATP and ADP equally well. In addition, and confirming the expectations, AMP is the ligand with weakest binding affinity. It is surprising that the N value for AMP is so much lower than 1. This deviation from the expected value could originate from an unexpected interference of the dialysis buffer in the protein state. ΔH values obtained for the three ligands show that the reaction promoted in these conditions is endothermic, absorbing energy to promote binding. In order to better understand the binding properties associated to the binding of the tested ligands to KtrA, as well as to confirm the presented values, these ITC experiments should be repeated. Varying protein and ligand concentrations could also be an interesting way of increasing the resolution of the measurements.

4.2. Characterization of KtrA mutants

A set of eight binding site residue mutants was obtained, with the main objective of understanding the importance of the mutated residues in the maintenance of protein's stability, functionality and conformation.

After analysing the KtrA structure, three promising binding pocket residues were chosen: the aspartic acid (D) in position 36 and the isoleucines (I) in positions 37 and 78. These residues are part of the core of the binding pocket where, by interacting with neighbouring residues, they create a cleft compatible for the binding of a ligand. Two different mutants were obtained by substituting the D36 residue for an asparagine (N) or a threonine (T). The change to an N resulted in a change in charge, with maintenance of its length, while the mutation to a T provoked the shortening of the residue, as well as loss of acidity. As for the nonpolar I residues, a mutation in position 37 to a T resulted in a length reduction and addition of a positive charge, while the substitution for a valine (V) in position 78 led to the shortening of the residue, with no change in the residue's hydrophobicity.

The arginine (R) residue in position 16 is particularly interesting since it seems to be the one that mediates the contraction of KtrA subunits during ATP binding by interacting simultaneously with the phosphate groups of both ATP molecules bound to the dimeric subunit. Such intercommunication does not happen when ADP is bound to KtrA (figure 11). By replacing this residue with an alanine (A) or a lysine (K), this effect is likely to disappear. These mutations result in physical modifications in the residue structure: a change to A leads to the shortening of the residue while the change to K results in a complete alteration in the residue orientation. The E residue also seems to coordinate the protein conformation by interacting selectively with the ligand phosphate groups. Its substitution for an A will result in a shorter residue in position 125, while the mutation to a glutamine (Q) promotes the alteration of the residue charge.

The cases of the mutants I78V and E125A are very interesting, since these soluble mutants underwent a change in the binding pocket sufficient to eliminate any affinity of the protein to ADP, failing to bind ADP-agarose. Although such affinity loss would be very interesting to evaluate, these mutant proteins could not be analysed due to the lack of a suitable purification method. Other purification methods for KtrA were already tested in the lab with unsuccessful results. Placing a histidine tag, for instance, at the N-terminus led to the

formation of inclusion bodies containing KtrA, while a fusion in the C-terminus led to the loss of stability. Therefore, although a lowering in the affinity to adenosine containing molecules is desired, it should still be high enough to allow the purification by elution with these ligands.

An interesting characteristic of tryptophan residues is their capacity to absorb radiation with a wavelength of 290nm and fluoresce [34]. The intensity of the fluorescence emitted by these residues varies according to the residue's surroundings and is a good indicator of conformational changes in those surroundings. It had been demonstrated in the lab that tryptophan fluorescence intensity dropped when ATP was bound to the wild type KtrA but not with ADP. This fluorescence change was correlated with the conformational change detected by X-ray crystallography. In this project, the tryptophan fluorescence was monitored to confirm the wild type protein results and to evaluate if similar changes were detected with the mutants. Confirming the previous observations, binding of ATP to the wild type protein resulted in a significant reduction of the fluorescence intensity while for ADP binding this tendency is not so accentuated. The mutants R16A and E125Q do not show significant differences between the two conditions, with both situations resulting in a slight drop in fluorescence intensity when compared to the ligand-free protein. These results could indicate the absence of conformational changes when the residues are mutated. Interestingly, the R16K mutant showed an apparent fluorescence increase with ligand binding. However, comparing the intensity levels for the two ligands does not reveal any significant difference between the two. The unusually low intensity recorded for the ligand-free protein could mean a dramatic change in the surroundings of tryptophan residues and, therefore, in the conformation, compared to the wild type protein.

The difference between the behaviour of R16A and R16K in the tryptophan fluorescence assay raises particular interest on what could be happening with both mutants. Understanding the binding properties of these two using ITC was the logical next step. During this project, the mutant E125Q was not submitted to ITC experiments, though it would be interesting to analyse the response of this mutant to ligand binding in the future.

After extensively dialysed in the same conditions as the wild type protein, the mutants R16A and R16K were titrated with ATP and ADP. The affinity for the ligands does not differ greatly between the two mutants, with the K_D values for ATP binding being of 769.23nM and 724.64nM for R16A and R16K respectively, and 1.55μM and 1.26μM, respectively also, for ADP binding. It is clear that substituting the amino acid 16 affects more the affinity for ADP than ATP indicating that the role of this residue is slightly more important for ADP binding than ATP. Similarly to what happened with the wild type protein, binding of both ATP and ADP to these mutant proteins is an endothermic reaction since ΔH values are negative.

Importantly, the N values obtained for the ITC titrations with these two mutants were suspiciously low. It is known that KtrA possesses one binding site per molecule [6]. If each site binds independently to one ligand molecule, the expected N value should be 1. However, this is not verified in this ITC data set. This deviation from the expected value could be originated from an unexpected interference of the dialysis buffer in the protein state. One possible explanation could be derived from the inactivation or destabilization of a fraction of KtrA in solution by the high phosphate concentrations, with the N values representing the

competent fraction in solution. The role of the phosphate groups in KtrA stabilization is clear and could lead to a "closing" of a percentage of binding sites, contributing, as well, to the lowering of N values. Another possible explanation would be the occurrence of errors when determining the ligand and protein concentrations. This assumption was discarded after determining the concentration values using multiple methods – Bradford protein assay, Direct Detect and conventional spectrometry – and repeating the titration assays.

As an alternative to the extensive dialysis with the D4 buffer, new ITC experiments were performed using the same mutants in an AMP saturated concentration in an HEPES-composed buffer at 15°C. Similar conditions were already used in the lab to explore the binding properties of the wild type protein to ATP (figure 19). In that experiment, a clear fit of 4 sequential binding sites (N = 4), each with different K_D values in the μM range, was observed. Given that KtrA organizes as an octamer in solution (four dimers), an N value like this one indicates that the 8 binding sites are not equivalent. This means that there is cooperativity between the binding sites, where binding of a ligand molecule to one binding site influences the binding affinity of the subsequent sites. As for the K_D values observed, these are higher than the ones determined for the protein dialysed with the D4 buffer. This is most likely due to binding competition with AMP.

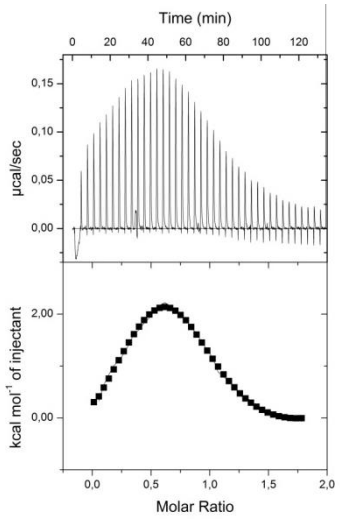

N = 4 binding sites

K_{D1} = 2.39 μM	K_{D2} = 34.72 μM
K_{D3} = 10.55 μM	K_{D4} = 11.19 μM
ΔH_1 = 297.6 cal/mol	ΔH_2 = 33600 cal/mol
ΔH_3 = -78650 cal/mol	ΔH_4 = 68780 cal/mol

Figure 19 - ITC data for KtrA WT saturated with 50 μM AMP in HEPES buffer. ATP was used as titrant. At the top of each graph is shown the raw ITC data and at the bottom the processed ITC curves. The binding sites per KtrA molecule, N, dissociation constants K_D, and enthalpy, ΔH, values are shown to the right of the graph. [Ricardo Pires data]

The ITC data obtained for R16A under these conditions is very similar to what was observed for the wild type protein. The same 4 sequential binding sites are detected in both ATP and ADP titrations, which means that the cooperativity is not altered. Overall, there does not seem to be any major difference in the binding affinities either for ATP or ADP binding to R16A, compared to the wild type protein, with the K_D values being in the μM range as well. However, the ATP titration does not reach a saturation plateau which means that this experiment should be repeated and the titrant volume should be increased in order to ensure saturation of the protein.

Surprisingly, the data regarding the mutant R16K is very different. The data was easily fitted with the simple model of a single binding site. The N values are very close to 1 (0.949

and 0.965 binding sites for ATP and ADP, respectively) indicating that the binding sites in this mutant are all equivalent. One can then infer that the specific mutation to a lysine in position 16 results in the loss of interdependency between binding sites. Another interesting observation is the high affinity to ATP binding, even higher than the value calculated for the wild type protein in D4 buffer. Considering that this was a competition experiment between the titrant ATP and AMP, one can only conclude that this mutant has a very high affinity towards ATP. In contrast, the affinity of this mutant for ADP is 40 fold lower than for ATP, with a K_D in the μM range. Unlike what was observed for the D4 dialysis buffer, the ΔH value is positive indicating that this competition reaction is exothermic. Similarly to the titration of R16A with ATP, the ADP titration data for R16K lacks a saturation plateau and therefore it will be necessary to repeat this experiment with larger titrant volumes.

Overall, the behaviour of both mutants during the competition assays was very different from what was observed for the extensively dialysed proteins in D4 buffer. Given these results, the suspicion around a possible interference associated with the phosphate buffer still stands and more experiments are required, possibly using the D2 buffer instead.

These data indicate that we are in the presence of a much more complex system than we originally expected. Understanding the ligand binding cooperative mechanism will provide new insight as to the functioning of the system and the way KtrAB is controlled by ATP and ADP binding.

As for the ligand removal method described in this project, a deeper understanding of the interference caused by the phosphate buffer is needed. New insight could arise from protein stability tests after extensive dialysis in D4 buffer, which could help define how this buffer affects protein stability. Furthermore, it would be interesting to determine the influence of the buffer in KtrA activity in the future. Repeating the ITC experiments with changing concentrations of the intervenient molecules would also allow a better understanding of the overall behaviour of the wild type protein, as well as the mutant proteins, upon ligand binding.

Chapter 5

Conclusions

In the present project, I proposed to assess the binding properties of KtrA to its higher-affinity ligands ATP and ADP. In order to accomplish this goal, however, a more urgent problem had to be addressed: a methodology to efficiently remove ligands bound to KtrA.

An extensive dialysis of the purified KtrA protein solution using a new phosphate-based dialysis buffer was developed. This methodology succeeded both in maintaining the KtrA stability in solution over time and in removing most of the ligand bound to the protein. However, after performing the ITC experiments with extensively dialysed protein, the stoichiometry parameters were unusually low, compared to the expected 1 binding site per KtrA molecule. This suggests that destabilization and inactivation of a fraction of protein in solution could arise from the extensive dialysis in the D4 buffer. These conclusions need to be further supported by repeating the ITC experiments. In the future, the stability of the protein after extensive dialysis in D4 buffer should be addressed, for instance, by analysing the melting temperature of the protein.

Nonetheless, the determined K_D values of KtrA to the ligands ATP, ADP and AMP were 690nM, 763nM and 4μM, respectively. These values can be considered with a high level of confidence since variations in the stoichiometry values do not interfere significantly with the affinity constants.

Of the mutants tested, I37T, R16A, R16K and E125Q are the ones that can undergo further characterization. Although promising, the mutants I37T and E125Q were not completely characterized in this project.

The binding of R16A and R16K to ATP did not differ from the WT when the proteins were extensively dialysed in D4 buffer. However, the affinity for ADP dropped slightly, with no difference between the mutants. Once again, the stoichiometry values were not convincing.

Surprisingly, when the protein was prepared and analysed in AMP-saturating conditions, it was possible to detect cooperativity between the binding sites of the KtrA. These same

results were observed for the mutant R16A. This reveals that the system considered may be more complex than originally thought.

In contrast, the R16K mutant does not present cooperative binding. In addition, this mutant displays very high affinity to ATP even under AMP-saturating conditions. These facts, allied to the clear difference relative to the wild type protein, indicate that this R16K should be further characterized either through determination of its structure or through biochemical and cell-based experiments where the functional impact of R16K KtrA mutant on the KtrAB activity is evaluated.

Further experiments are needed in order to confirm the conclusions drawn here. Since D2 buffer presented acceptable compatibility to KtrA, it would be interesting to repeat the ITC experiments with protein dialysed using this buffer. Another interesting line of experiments would be to assess the binding properties of ATP and ADP for the KtrAB complex and compare them to the ones observed for KtrA alone.

In the future, experiments with mixing ATP and ADP concentrations should be made in order to understand how variations on ATP/ADP ratios influence the activation of the KtrAB system.

References

1. Corratge-Faillie, C., et al., *Potassium and sodium transport in non-animal cells: the Trk/Ktr/HKT transporter family.* Cell Mol Life Sci, 2010. **67**(15): p. 2511-32.
2. Rodriguez-Navarro, A., *Potassium transport in fungi and plants.* Biochim Biophys Acta, 2000. **1469**(1): p. 1-30.
3. Nakamura, T., et al., *KtrAB, a new type of bacterial K(+)-uptake system from Vibrio alginolyticus.* J Bacteriol, 1998. **180**(13): p. 3491-4.
4. Hanelt, I., et al., *KtrB, a member of the superfamily of K+ transporters.* Eur J Cell Biol, 2011. **90**(9): p. 696-704.
5. Durell, S.R., et al., *Evolutionary Relationship between K+ Channels and Symporters.* Biophysical journal, 1999. **77**(2): p. 775-788.
6. Vieira-Pires, R.S., A. Szollosi, and J.H. Morais-Cabral, *The structure of the KtrAB potassium transporter.* Nature, 2013. **496**(7445): p. 323-8.
7. Durell, S.R. and H.R. Guy, *Structural models of the KtrB, TrkH, and Trk1,2 symporters based on the structure of the KcsA K(+) channel.* Biophys J, 1999. **77**(2): p. 789-807.
8. Tholema, N., et al., *All four putative selectivity filter glycine residues in KtrB are essential for high affinity and selective K+ uptake by the KtrAB system from Vibrio alginolyticus.* J Biol Chem, 2005. **280**(50): p. 41146-54.
9. Tholema, N., et al., *Change to alanine of one out of four selectivity filter glycines in KtrB causes a two orders of magnitude decrease in the affinities for both K+ and Na+ of the Na+ dependent K+ uptake system KtrAB from Vibrio alginolyticus.* FEBS Lett, 1999. **450**(3): p. 217-20.
10. Maser, P., et al., *Glycine residues in potassium channel-like selectivity filters determine potassium selectivity in four-loop-per-subunit HKT transporters from plants.* Proc Natl Acad Sci U S A, 2002. **99**(9): p. 6428-33.
11. Bossemeyer, D., et al., *K+-transport protein TrkA of Escherichia coli is a peripheral membrane protein that requires other trk gene products for attachment to the cytoplasmic membrane.* J Biol Chem, 1989. **264**(28): p. 16403-10.
12. Roosild, T.P., et al., *A mechanism of regulating transmembrane potassium flux through a ligand-mediated conformational switch.* Cell, 2002. **109**(6): p. 781-91.
13. Roosild, T.P., et al., *KTN (RCK) domains regulate K+ channels and transporters by controlling the dimer-hinge conformation.* Structure, 2009. **17**(6): p. 893-903.
14. Haro, R. and A. Rodriguez-Navarro, *Molecular analysis of the mechanism of potassium uptake through the TRK1 transporter of Saccharomyces cerevisiae.* Biochim Biophys Acta, 2002. **1564**(1): p. 114-22.
15. Albright, R.A., K. Joh, and J.H. Morais-Cabral, *Probing the structure of the dimeric KtrB membrane protein.* J Biol Chem, 2007. **282**(48): p. 35046-55.
16. Holtmann, G., et al., *KtrAB and KtrCD: two K+ uptake systems in Bacillus subtilis and their role in adaptation to hypertonicity.* J Bacteriol, 2003. **185**(4): p. 1289-98.
17. Murata, T., et al., *The ntpJ gene in the Enterococcus hirae ntp operon encodes a component of KtrII potassium transport system functionally independent of vacuolar Na+-ATPase.* J Biol Chem, 1996. **271**(17): p. 10042-7.
18. Matsuda, N., et al., *Na+-dependent K+ uptake Ktr system from the cyanobacterium Synechocystis sp. PCC 6803 and its role in the early phases of cell adaptation to hyperosmotic shock.* J Biol Chem, 2004. **279**(52): p. 54952-62.
19. Kroning, N., et al., *ATP binding to the KTN/RCK subunit KtrA from the K+ -uptake system KtrAB of Vibrio alginolyticus: its role in the formation of the KtrAB complex and its requirement in vivo.* J Biol Chem, 2007. **282**(19): p. 14018-27.
20. Albright, R.A., et al., *The RCK domain of the KtrAB K+ transporter: multiple conformations of an octameric ring.* Cell, 2006. **126**(6): p. 1147-59.

21. Jiang, Y., et al., *Crystal structure and mechanism of a calcium-gated potassium channel*. Nature, 2002. **417**(6888): p. 515-22.
22. Hanelt, I., et al., *Gain of function mutations in membrane region M2C2 of KtrB open a gate controlling K+ transport by the KtrAB system from Vibrio alginolyticus.* J Biol Chem, 2010. **285**(14): p. 10318-27.
23. Chazan, A. *Peptide Property Calculator*. [cited 2014 12-06-2014]; Available from: http://www.basic.northwestern.edu/biotools/proteincalc.html.
24. Schlosser, A., et al., *NAD+ binding to the Escherichia coli K(+)-uptake protein TrkA and sequence similarity between TrkA and domains of a family of dehydrogenases suggest a role for NAD+ in bacterial transport*. Mol Microbiol, 1993. **9**(3): p. 533-43.
25. Dong, J., et al., *Structures of the MthK RCK domain and the effect of Ca2+ on gating ring stability.* J Biol Chem, 2005. **280**(50): p. 41716-24.
26. Bennett, B.D., et al., *Absolute metabolite concentrations and implied enzyme active site occupancy in Escherichia coli.* Nat Chem Biol, 2009. **5**(8): p. 593-9.
27. Radchenko, M.V., J. Thornton, and M. Merrick, *Control of AmtB-GlnK complex formation by intracellular levels of ATP, ADP, and 2-oxoglutarate*. J Biol Chem, 2010. **285**(40): p. 31037-45.
28. Jiang, P. and A.J. Ninfa, *Escherichia coli PII signal transduction protein controlling nitrogen assimilation acts as a sensor of adenylate energy charge in vitro.* Biochemistry, 2007. **46**(45): p. 12979-96.
29. Clark, J. *The Beer-Lambert Law*. 2007 [cited 2014 15-06-2014]; Available from: http://www.chemguide.co.uk/analysis/uvvisible/beerlambert.html.
30. Sigma-Aldrich, *Adenosine 5'-triphosphate disodium salt, Product Information* Sigma-Aldrich, Editor.
31. Velazquez-Campoy, A., et al., *Isothermal titration calorimetry*. Curr Protoc Cell Biol, 2004. **Chapter 17**: p. Unit 17 8.
32. Promega, *ENLITEN ATP Assay System Bioluminescence Detection Kit for ATP Measurement*, P. Corporation, Editor 2009.
33. Ladbury, J.E. and M.L. Doyle, *Biocalorimetry 2 : applications of calorimetry in the biological sciences*. 2004, Chichester ; Hoboken, NJ: Wiley. xv, 259 p.
34. Vivian, J.T. and P.R. Callis, *Mechanisms of tryptophan fluorescence shifts in proteins.* Biophys J, 2001. **80**(5): p. 2093-109.

Appendix

A.1. Example of an anion-exchange profile correspondent to KtrA elution upon a crescent KCl concentration gradient. In the yy axis is represented the radiation intensity detected upon incidence of 280nm UV radiation, correspondent to the protein eluted, while the xx axis depicts the elution volume. Protein elution from anion-exchange column happens as the protein bound is substituted by the anion Cl^- in solution. The fractions comprised between the 8^{th} and the 16^{th} ml, corresponding to stable KtrA, were pooled and further processed.

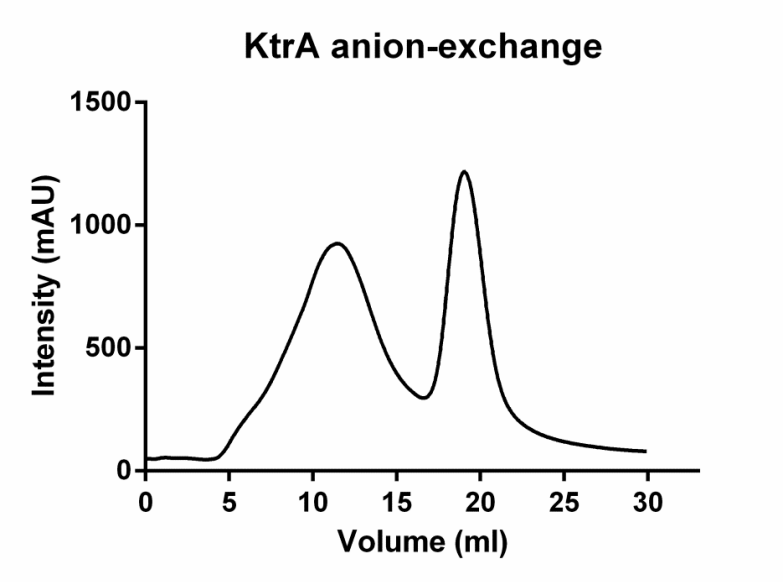

A.2. Example of a size-exclusion chromatography profile correspondent to KtrA purification. In the yy axis is represented the radiation intensity detected upon incidence of 280nm UV radiation, correspondent to the protein eluted, while the xx axis depicts the elution volume. The size of the molecules in solution dictates the volume at which they are eluted from the Superdex S200 column (25 ml). The KtrA in solution elutes at around 12.5 ml. By pooling the peak around this volume, a purified protein solution in Gel Filtration buffer is obtained. The ligand molecule used to elute KtrA from the ADP-agarose resin elutes from the size-exclusion column at around 20 ml.

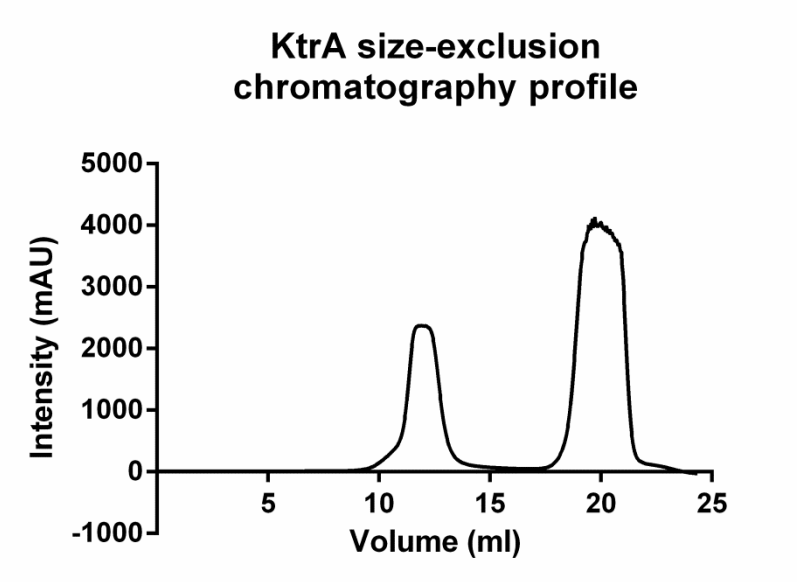

A.3. Example of a Direct Detect Analysis Results Report. The blank was set using protein-free Gel Filtration buffer. The samples analysed were an ATP-eluted KtrA solution; a 2 times dilution of the same solution; and an AMP-eluted KtrA solution. All the protein solutions were previously purified by size-exclusion chromatography.

Direct Detect™
Analysis Results Report

Date / Time :	3/24/2014 5:57:34 PM	**Instrument Serial # :**	M100061
Card Name :	Sample1	**Software Version :**	2.0.0.28
User Name :	Operator	**Company Name :**	
Protein Method :		**Department :**	
Lipids Method :		**Location :**	
Number of Reads :	1	**Spectral Plot :**	Raw Data
Diagnostics :	Test expired		
Messages :			

Sample Pos		Type	Sample Name	Protein []
4		Sample	KtrA-AMP	1.783
3		Sample	KtrA-ATP dil	1.134
2		Sample	KtrA-ATP	2.004
1		Blank	Gel Filtration buffer	----

[My Documents]\Direct Detect\Spectra\Operator\20140324\175734\KtrA-AMP.4.0
[My Documents]\Direct Detect\Spectra\Operator\20140324\175734\KtrA-ATP dil.3.0
[My Documents]\Direct Detect\Spectra\Operator\20140324\175734\KtrA-ATP.2.0
[My Documents]\Direct Detect\Spectra\Operator\20140324\175734\Gel Filtration buffer.1